

Using fibrinogen barriers to restrict the motion of shear-driven supported lipid bilayers

Master of Science Thesis in Biomedical Engineering

THOMAS OLSSON

Department of Applied Physics
Division of Biological Physics
CHALMERS UNIVERSITY OF TECHNOLOGY
Göteborg, Sweden, 2011
Report No.2011:06

THESIS FOR THE DEGREE OF MASTER OF SCIENCE

Using fibrinogen barriers to restrict the motion of shear-driven supported lipid bilayers

THOMAS OLSSON



CHALMERS

Department of Applied Physics
CHALMERS UNIVERSITY OF TECHNOLOGY
Göteborg, Sweden 2011

Using fibrinogen barriers to restrict the motion of shear-driven supported lipid bilayers

THOMAS OLSSON

© THOMAS OLSSON, 2011.

Technical report no 2011:06
Department of Applied Physics
Chalmers University of Technology
SE-412 96 Göteborg
Sweden
Telephone + 46 (0)31-772 1000

Cover Image: A shear-driven supported lipid bilayer moving inside a channel with fibrinogen barriers on either side, showing accumulation of fluorescently-labeled molecules at the bilayer front.

Printed at Chalmers Reproservice
Göteborg, Sweden 2011

Using fibrinogen barriers to restrict the motion of shear-driven supported lipid bilayers

THOMAS OLSSON

Department of Applied Physics
Chalmers University of Technology

Abstract

About 70% of all drug targets are proteins situated in the cell-membrane. However, the cell-membrane offers a very complex environment in which to study just a single type of interaction with a specific type of protein, being made up of hundreds of different lipids, over 200 different proteins and oligosaccharides. There exist for this reason some different simplified models of cell membranes, where only the base of the cell-membrane is used, a bilayer often made up of just one type of lipids. A certain protein could then be incorporated into the lipid bilayer and be studied. One simplified model of the cell-membrane is a supported lipid bilayer, which is a lipid bilayer formed on a solid support. SLBs, which is the model used in this work, are formed in microfluidic channels, due to the high level of controllability it offers with laminar flows, but also requiring only small quantities of samples. It was shown by Jönsson et. al that an SLB could be made to move in a desired direction in the microfluidic channel, by having a relatively high bulk flow in the channel above the formed SLB. This proved very useful as molecules incorporated into an SLB was shown to accumulate at the front of the moving bilayer, an increasing concentration of for example a certain protein to be studied means an increase in signal strength. An increase in signal strength could for example mean that things could be studied which would otherwise drown in noise due to too low concentrations. A microfluidic channel is made of glass and PDMS, both materials on which SLBs can form. This means that an SLB when moving along the channel floor could also start moving up along the walls of the channels, thus taking with it incorporated molecules which could have been accumulated at the front. In a microfluidic channel the flow profile is such that bulk flow velocity is highest in the middle of the channel and goes down to zero at the walls, this reduce the effectiveness of the accumulation as some accumulated molecules close to the walls are continuously left behind. Fibrinogen is a protein which with the right conditions could be made to adsorb densely on the channel surface. When fibrinogen is densely packed, it forms a barrier stable enough to restrict the motion of a moving SLB. Fibrinogen barriers are studied within this work as a means of constricting the moving SLB to the center of the microfluidic channel in order to stop it from moving up the channel walls and also to increase the effectiveness of the accumulation as the zero bulk flow regions are avoided. Some results from this study are that fibrinogen indeed can form a barrier dense enough to withstand a moving bilayer, and that accumulation at the front is more effective when fibrinogen barriers are used.

Keywords: Supported Lipid bilayers, microfluidics, fluorescence microscopy, shear-driven

Contents

List of abbreviations	v
1 Introduction	1
2 Theory	2
2.1 Lipids	2
2.1.1 Fluorescently labeled lipids	3
2.2 Supported Lipid Bilayers.....	4
2.2.1 SLB formation.....	4
2.3 Shear-driven lipid bilayer	5
2.3.1 Accumulation of molecules incorporated into the SLB	6
2.4 Barriers used with SLBs	7
2.5 Fibrinogen	8
2.6 Microfluidics.....	8
2.7 Properties of fibrinogen barriers and their effect on a shear driven SLB.....	10
3 Method	11
3.1 Materials.....	11
3.2 Fabricating microfluidic channels	12
3.3 Flow regulation in the microfluidic system	12
3.4 Experimental preparations	13
3.5 Forming a bilayer in a microfluidic channel.....	15
3.5.1 Driving an SLB with a shear force	16
3.6 Forming fibrinogen barriers in a microfluidic channel.....	16
3.7 Inverted microscope and camera	17
3.8 Fluorescence Recovery After Photobleaching (FRAP)	18
4 Results & Discussion	19
4.1 Properties of the fibrinogen barrier.....	19
4.1.1 Effects of diffusion on fibrinogen barrier formation	22
4.1.2 Fibrinogen might bind to an SLB	25
4.2 Comparisons of driving a bilayer with or without a fibrinogen barrier	26
4.2.1 Velocity of SLB front.....	26
4.2.2 Accumulation of fluorescently labeled lipids	28

5	Conclusion and Outlook	31
	Acknowledgements	35
	References	36
	Appendix A - Manufacturing microfluidic channels	38
	Appendix B - Preparation of lipid vesicles	40
	Appendix C - Switching used in the experiments	41

List of abbreviations

FRAP	Fluorescence Recovery After Photobleaching
PDMS	Polydimethylsiloxane
POPC	1-palmitoyl-2-oleoyl- <i>sn</i> -glycero-3-phosphatidylcholine
QCM	Quartz Crystal Microbalance
R-DHPE	Lissamine rhodamine B 1,2-dihexadecanoyl- <i>sn</i> -glycero-3-phosphatidylethanolamine
SDS	Sodium dodecyl sulfate
SLB	Supported Lipid Bilayer

1 Introduction

Cell-membranes are interesting to study for various reasons as they regulate what is allowed in and out of the cell. Cell-membranes consist of a lipid bilayer made up of about hundred different types of lipids and are functionalized with many sorts of incorporated proteins and also different oligosaccharides[1], see figure 1.1. Membrane incorporated proteins allow for transport of specific molecules and ions which could otherwise not pass through the membrane[2]. About 70% of all pharmaceutical compounds targets membrane proteins[3, 4]. Given its many constituents, the cell-membrane itself provide a complex environment to study and it is in many cases preferable to work with a simplified model such as a Supported Lipid Bilayer (SLB), which for example could be functionalized with some protein of interest. An SLB is a model which provides an environment which is relatively close to the proteins native one. One of the benefits with using an SLB instead of a natural membrane when it comes to proteins is the possibility to pack them more densely in the SLB which is done to increase the signal strength of some measurable property.

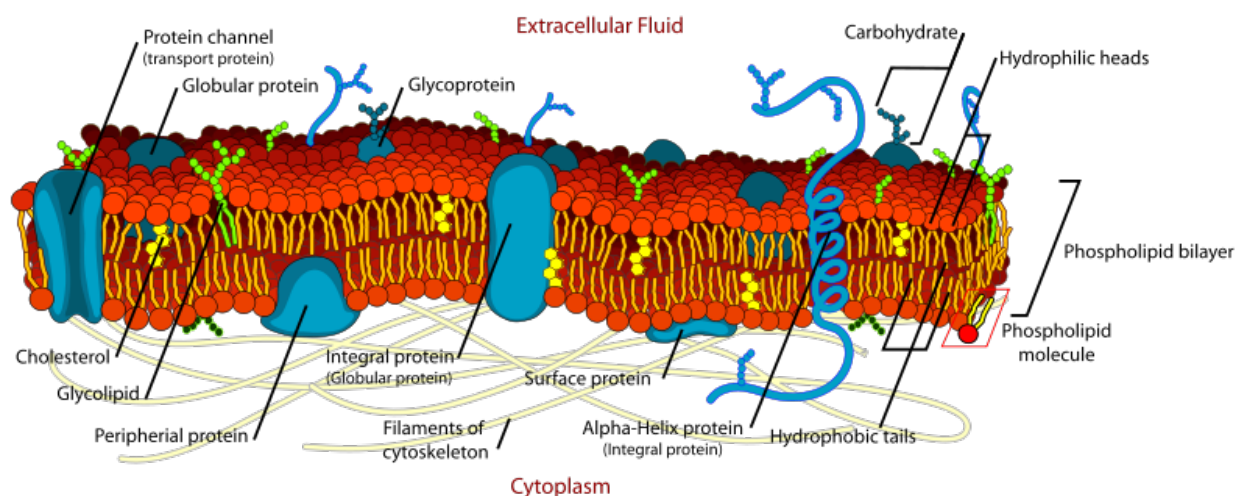


Figure 1.1 Sketch of a cell-membrane. Figure from http://cellbiology.med.unsw.edu.au/units/images/Cell_membrane.png

Recently Jönsson et al. described a new technique in which a bulk flow is used over the SLB to induce a shear force in the SLB, which drives it in the direction of the flow[5]. It was shown that the SLB under these circumstances move with a rolling motion, so that the bottom leaflet is almost immobile while the upper moves. It was also discovered that molecules incorporated into the SLB had a tendency not to follow the roll down into the lower leaflet but instead accumulate at the front of the SLB [5, 6]. Different kinds of accumulated molecules could then be separated by applying a reversed flow[6]. Due to the bulk flow profile, the shear force acting on the SLB is higher in the middle of the channel and close to zero at the walls[7, 8]. Because of this the accumulation and separation profiles tend to be smeared out (parabolic), which leads to both reduced accumulation and separation. This work will focus on forming fibrinogen barriers for the

SLB close to the microfluidic channel walls. The aim of this is twofold, by confining the SLB to the center of the channel it cannot spread up onto the walls and the SLB is also kept out of the zero bulk flow region close to the channel walls which in turn significantly increase accumulation and separation of membrane associated molecules. Improved accumulation and separation is an important step towards future applications of shear-driven SLBs. One potential application is incorporation of natural cell membrane fragments into the SLB[9]. Proteins that are naturally sparsely situated in the cell-membrane could first be accumulated and then separated. Any membrane-associated proteins could be accumulated in such concentrations that a measurable signal could be detected upon a specific binding to these proteins (which otherwise might not be observed). An SLB with all membrane associated proteins separated into well-defined regions could be used for screening purposes to study specific membrane protein-ligand interactions. Protein-ligand interactions are studied by the pharmaceutical companies in order to find new medicines.

So, future applications looks promising, but this study deal mainly with the formation of fibrinogen barriers and how these affect a shear-driven SLB.

2 Theory

2.1 Lipids

Lipids are made up of a hydrophilic (likes water) head group and a hydrophobic (dislikes water) tail region [2], see figure 2.1.

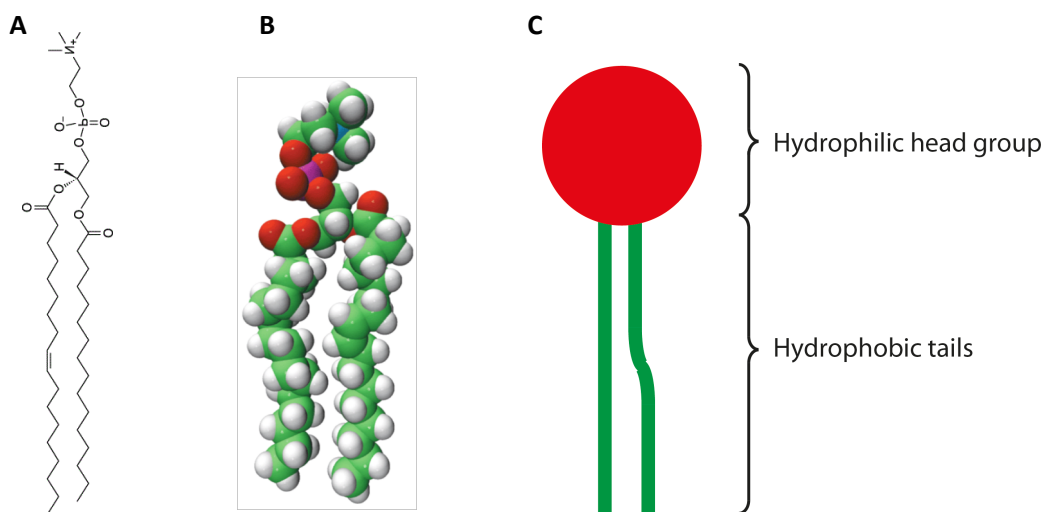


Figure 2.1. POPC (A) Chemical structure, (B) space-filling model and (C) simplified sketch. Figure A and B are from Avanti Lipids.

This property makes the lipids, when in an aqueous environment, self-assemble into different structures in order to mask their hydrophobic parts from the aqueous environment in this way minimizing the free energy[1]. Based on the geometrical shapes of the lipids, some types of lipids

with a conical geometrical structure form micelles[1], while other types like the phospholipids with a cylindrical geometrical structure used in this work forms double layered bilayer vesicles in an aqueous solution[1], see figure 2.2.

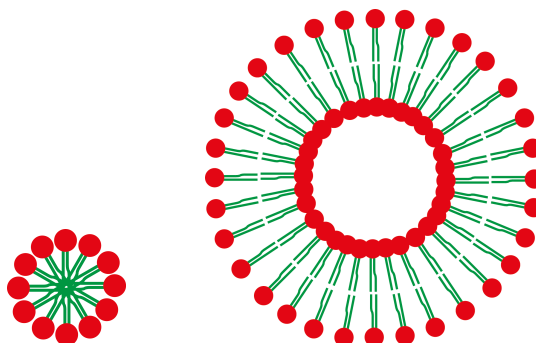


Figure 2.2. Left panel: Lipids forming a micelle. Right panel: Lipids forming a bilayered lipid vesicle.

2.1.1 Fluorescently labeled lipids

In order to be able to detect lipid vesicles and formed SLBs in fluorescence microscopy, some of the lipids are marked with a fluorescent molecule. In this work rhodamine was used as a marker in all experiments, see figure 2.3. Rhodamine is a fluorescent molecule with an excitation maxima at a wavelength of about 560 nm[10]; once an electron has been excited it emits light of another wavelength on its way back to the ground state, where the emission has a maxima of about 580 nm [10].

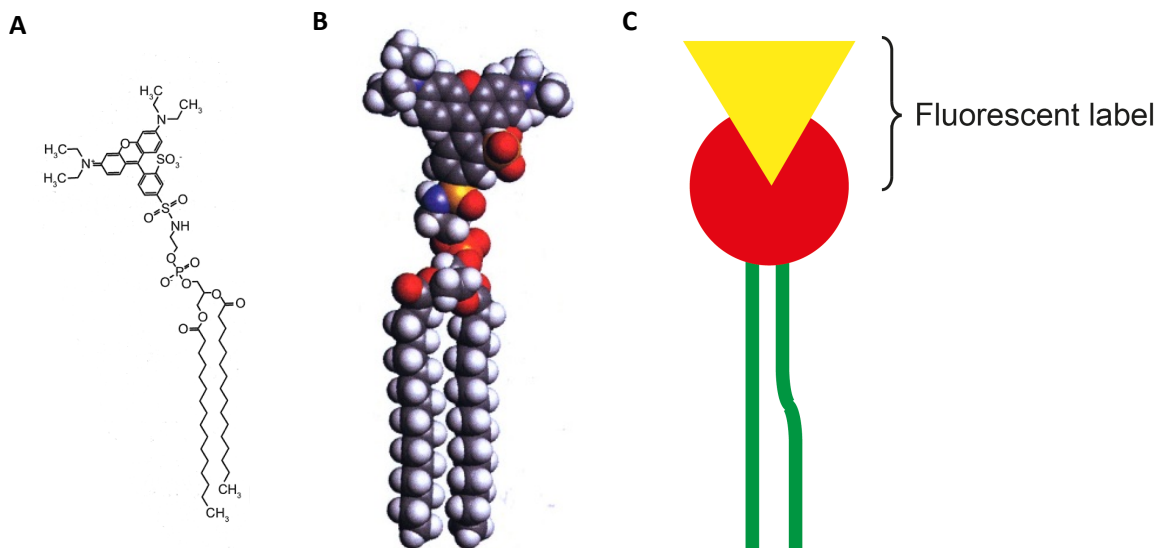


Figure 2.3. R-DHPE (A) Chemical structure, (B) space-filling model and (C) a simplified sketch. Figure A and B are from [11].

2.2 Supported Lipid Bilayers

Cell membranes consist of hundreds of different kinds of lipids, membrane-associated proteins and sugars [1]. Phosphatidylcholine is the most common phospholipid in human cell membranes [2], and POPC, which is a phosphatidylcholine, was used in this work to form SLBs. Because cell-membranes offers such a complex environment, when introducing some molecules into the solution surrounding the cell-membrane with a specific membrane-associated molecule target in mind, the molecules introduced might well interact with other membrane-associated molecules as well. This means that the measured signal might have more dependencies than the one intended for study. Another downside of using natural cell-membranes is that the membrane associated molecules intended for study might not be densely enough situated in the cell-membrane for a signal to be possible to acquire. SLBs on the other hand offer a more controllable environment and also an environment where targets can be accumulated densely enough to achieve a good signal. Simplified models of cell-membranes are very useful when it comes to characterization of the kinetics between a certain membrane-associated protein for example and a specific ligand.

2.2.1 SLB formation

As a vesicle solution is flown over a surface the vesicles within it diffuse in all directions due to Brownian motion and if vesicles come close enough to a surface they can adsorb onto it due to electrostatic interaction, resulting in a slight flattening of the lipid vesicles. Once the vesicle coverage reaches a critical point, the vesicles rupture in a chain reaction and form a planar bilayer consisting of two sheets of lipids, see figure 2.4.

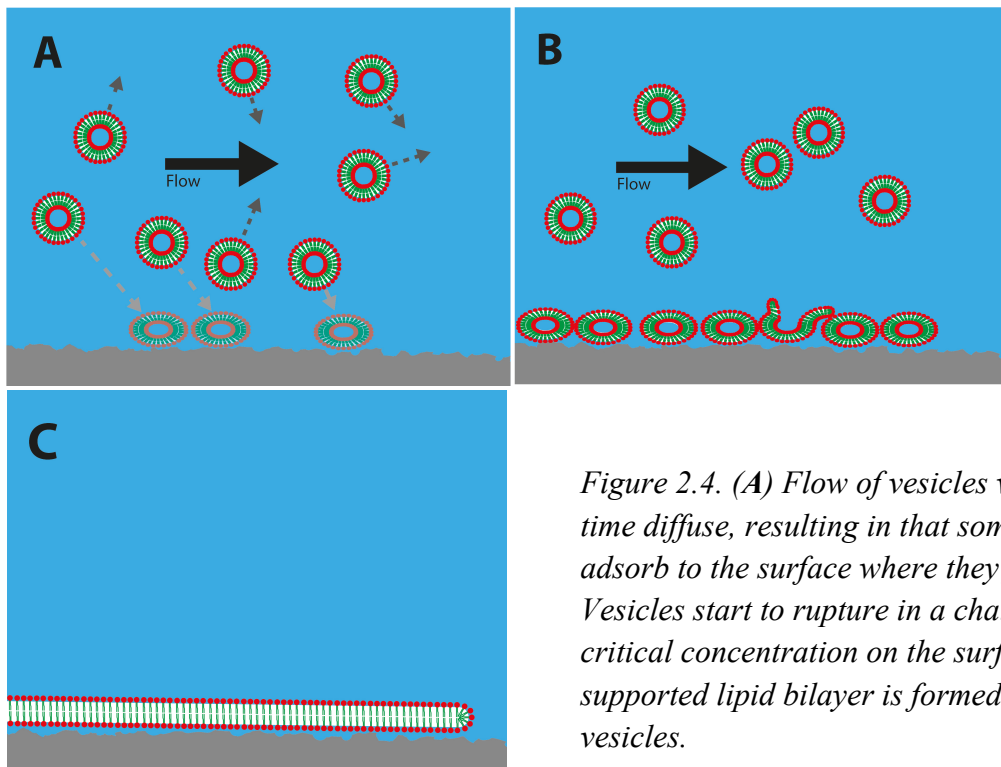


Figure 2.4. (A) Flow of vesicles which at the same time diffuse, resulting in that some reach and adsorb to the surface where they flatten slightly (B) Vesicles start to rupture in a chain reaction at a critical concentration on the surface. (C) A supported lipid bilayer is formed from the ruptured vesicles.

There are only a few different materials on which SLBs can form such as glass, SiO₂, mica, oxidized PDMS and some soft polymers[12, 13]. On other materials like metals, vesicles adsorb at different rates but do not rupture[13].

In order to study an SLB driven with a shear force, it is important to know some of its characteristics. An SLB is about 5 nm thick [14, 15] and the distance between the SLB and the support is about 1 nm [14, 16], see figure 2.5. Lipids diffuse freely within their leaflets which is called lateral diffusion, also lipids switching from one leaflet to the other occur but at a much longer time scale(hours to days)[17].

2.3 Shear-driven lipid bilayer

The bulk flow induces a shear-force σ_{hydro} in the SLB which is proportional to the bulk flow velocity, the bulk flow is at its highest at the center of the microfluidic channel and goes down to zero close to the walls of the channel[17]. The SLB moves like the wheels of a tank describing a rolling motion, see figure 2.8. The lower monolayer remains almost still while the upper monolayer moves and so the SLB spread with the direction of the bulk flow. When the SLB moves there is a frictional force between the interfaces of the two monolayers with a resulting frictional force of $b(v_{\text{upper}} - v_{\text{lower}})$. There is also a frictional force between the lower monolayer and the support $b_{\text{ls}} \cdot v_{\text{lower}}$ [7]. The hydrodynamic force exerted on molecules incorporated into the SLB is higher as they stick up further into the bulk flow. This have been used previously in order to separate different kinds of molecules that have accumulated at the SLB front by reversing the bulk flow, based on the molecular size these molecules experience different hydrodynamic forces and thus moves at different rates[6]. It has also been shown that shear-driven SLBs could be used to suspend SLBs over sub micrometer sized wells[18], which could be useful for example when studying transport across lipid bilayers.

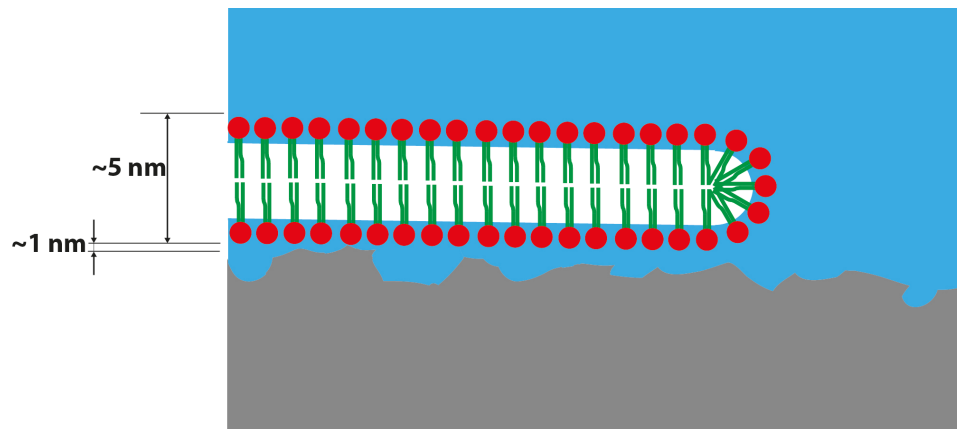


Figure 2.5. An SLB is about 5 nm thick, with a distance to the supporting surface of about 1 nm.

The bulk flow is as mentioned before highest in the center of the microfluidic channel, and the flow rate is proportional to the shear-force acting on the SLB, see figure 2.6. This property combined with a slight deformation of the PDMS channel together with line tension and accumulation at the SLB front of incorporated molecules are the reasons why the curvature look the way it does[17]. Another way a bilayer could move is through self-spreading. An SLB formed in a reservoir will due to bilayer-surface interaction self-spread and could be made to move along a channel, but at a fraction of the velocity by which an SLB move during a high bulk flow.

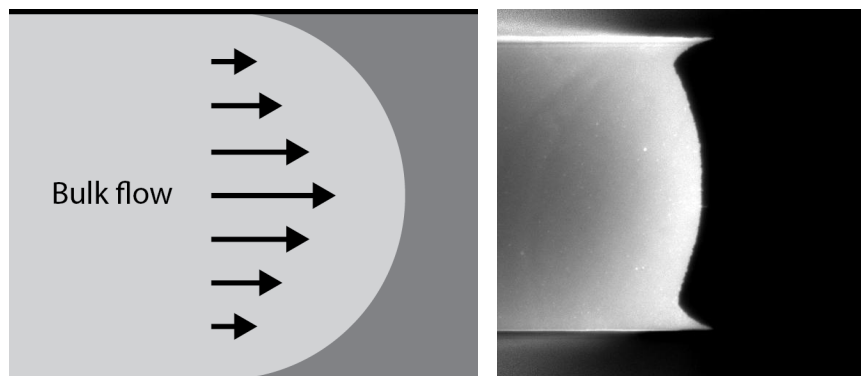


Figure 2.6. Left panel: Top view of the bulk flow profile of an SLB moving over the surface of the channel. Right panel: Fluorescence image of SLB moving in channel.

2.3.1 Accumulation of molecules incorporated into the SLB

The SLB describes a rolling motion when it moves forward in a microfluidic channel, it would seem that in the most cases studied, molecules incorporated into the SLB are unable to follow the rolling motion of the front down into the lower sheet and therefore accumulate at the front as shown in [5], see also figure 2.8. The distance between the SLB and the support is as mentioned earlier $\sim 1\text{nm}$, and in the case of rhodamine labeled lipids, the rhodamine headgroup is too large to fit between the SLB and the support. Molecules incorporated into the SLB also move independently from the SLB motion, naturally by diffusion and due to the hydrodynamic force from the flow, the latter also contributes to the accumulation at the front of the SLB.

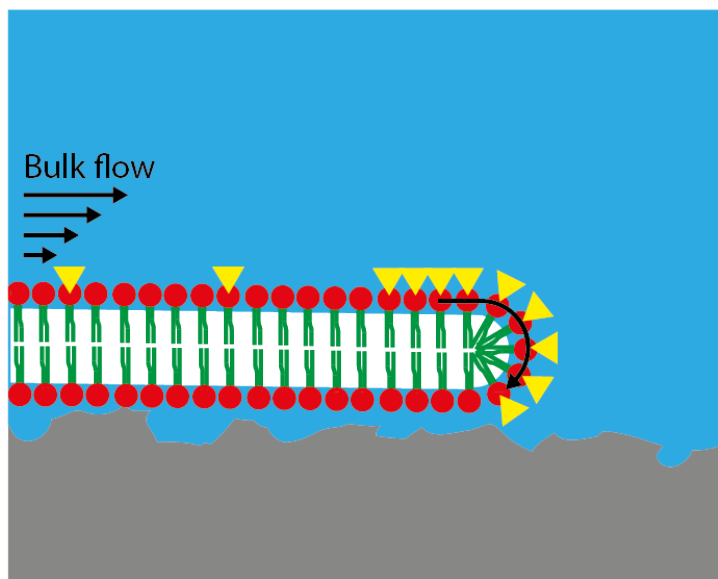


Fig 2.8. Illustration of an SLB with some lipids labeled with a fluorescent molecule. These molecules cannot pass from the upper sheet to the lower; this makes them accumulate at the front of the SLB.

A different method used for accumulation is to apply an external electric field (electrophoresis) [19], but this could only be used to accumulate charged molecules, while shear-driven accumulation will also accumulate uncharged ones. Another method of accumulating membrane incorporated molecules that has been used is to accumulate against a barrier[9].

2.4 Barriers used with SLBs

Different types of barriers have been used to restrict SLBs, one type is different kinds of mechanical scratchings either before or after a bilayer has been formed[19]. The scratching could for example be performed with a pair of tweezers, but an SLB might overcome the scratch unless it has sufficiently sharp edges[12]. Another kind of technique used to create barriers is blotting, an SLB is formed and a PDMS stamp with a profile is pressed against it and lifted, thus removing the SLB in a pattern[20]. A third technique is to pre-pattern the surface either with aluminium oxide or gold using lithography[21], or by adsorption of molecules that could bind strongly enough to the substrate, but on which no SLB would form[22]. The last technique seem to be the most suitable to use together with the kind of microfluidic channel used in this work.

2.5 Fibrinogen

Fibrinogen is a glycoprotein found in the blood plasma at 2.5-4 mg/ml[23]. Its length is about 45 nm and its width ~7 nm[24-26], see figure 2.9. Thrombin turns fibrinogen into fibrin which is a part of the process by which blood clots[27]. In this work fibrinogen is adsorbed to a glass substrate surface in order to form a barrier for a shear driven SLB, fibrinogen has been used with this purpose in previous work[22]. Different parameters like concentration, buffer pH and the flow rates effect on fibrinogen adsorption on substrate surface in microfluidic channels has previously been investigated[28]. There it was found that maximum adsorption occurred at fibrinogen concentrations ≥ 50 $\mu\text{g/ml}$, at buffer ionic strengths of ~ 0.8 mM, at a pH 5 which is close to the isoelectric point of fibrinogen (at pH 5.5, where it has no net charge) and at low flow rates >0 up to $1 \mu\text{l/min}$. The strongest driving force for fibrinogen adsorption was thought to be ionic interactions, hydrophobic interactions and van der Waals forces.

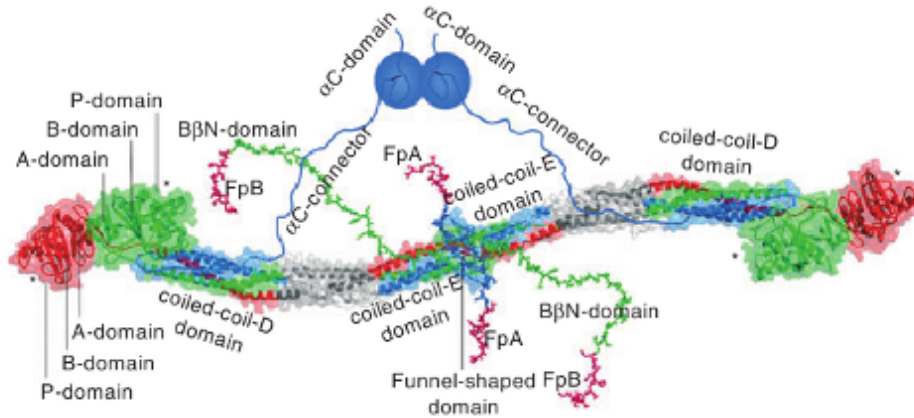


Figure 2.9. Structure of human fibrinogen, figure from <http://faculty.uml.edu/vbarsegov/research/fibers.html>

2.6 Microfluidics

The great advantage of using a micro fluidic channel, apart from requiring smaller sample volumes, is that it makes it possible to have a very high control when injecting solutions into the system as solutions in a micro sized environment have a laminar flow[29]. Laminar flow means that there's no presence of turbulence within the system and so when solutions are injected simultaneously into a micro sized channel they do not mix. The cross-sectional dimensions are crucial in order to obtain a laminar flow. The channels used in this work had a channel width of $150 \mu\text{m}$ and a channel height of $113 \mu\text{m}$, see figure 2.10 left panel.

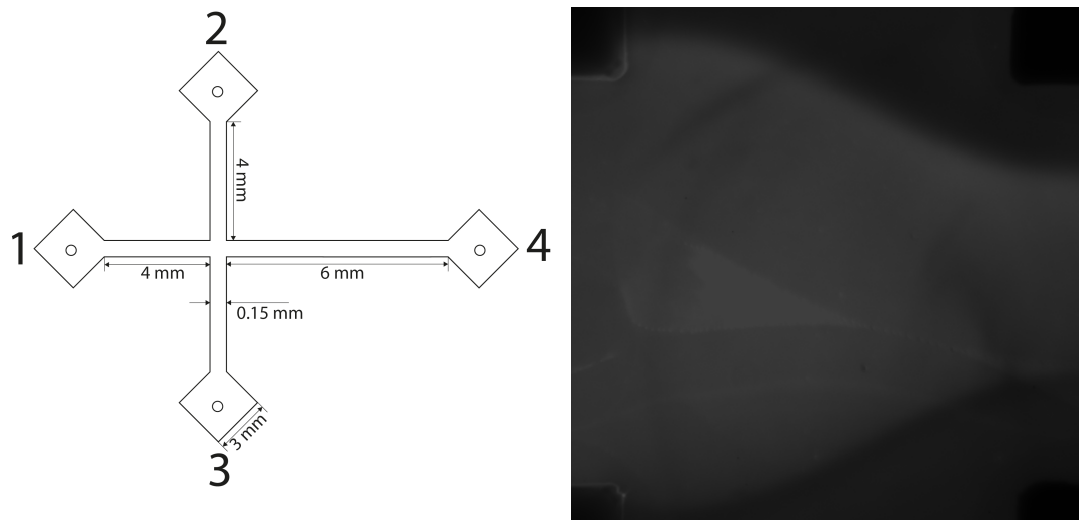


Figure 2.10. Left panel: A sketch of the microfluidic channel (not to scale). Right panel: Fibrinogen injected at the same time as buffer in the microfluidic channel.

The case shown in figure 2.10 right panel is when fibrinogen is injected in through the upper and lower arm of the channel at 10 $\mu\text{l}/\text{min}$, at the same time buffer pH 5 is injected through the left arm at 50 $\mu\text{l}/\text{min}$ while the right arm is used as outlet. An SLB had previously been formed in the channel and prior to fibrinogen injection all of the SLB had same fluorescence, but in regions where fibrinogen solution passes over the SLB it darkens. The sharp contrast between areas with a buffer flow in comparison to the ones with fibrinogen, as well as the clear symmetry between upper and lower injection patterns, both show that there is no turbulence present and that the solutions do not mix apart from diffusion.

2.7 Properties of fibrinogen barriers and their effect on a shear driven SLB

During SLB formation there is not only adsorption on the glass surface but there is also adsorption on the PDMS walls and roof of the channel where the vesicles are injected. However, in the opposite side of the channel from where the SLB is formed, there is no adsorption on the PDMS walls and roof as no vesicles have passed this location. When driving the SLB with a shear force into the right hand side of the 4-arm channel there has been noticed that the SLB in some cases moves up along the PDMS walls and even up unto the roof of the channel [17]. This results in a less controlled system and one of the main purposes of using fibrinogen barriers is to prevent the SLB from both reaching and move up along the walls of the PDMS channel as it is pushed. Perhaps even more importantly, the fibrinogen barriers confine the SLB to the center of the channel where the shear forces are more even.

From Bernuolli's theorem for an incompressible fluid the equation of continuity is expressed as $A_1 \cdot v_1 \cdot \Delta t = A_2 \cdot v_2 \cdot \Delta t$, where A is the cross sectional area of a channel, v is the velocity of the fluid and Δt is a time step[30]. An SLB can in these experiments be seen as a two-dimensional incompressible liquid and hence instead of having a cross sectional area A , the expression could be written as $S_1 \cdot v_1 \cdot \Delta t = S_2 \cdot v_2 \cdot \Delta t$, where S is the width of the channel along which the SLB is moving, see figure 2.11.

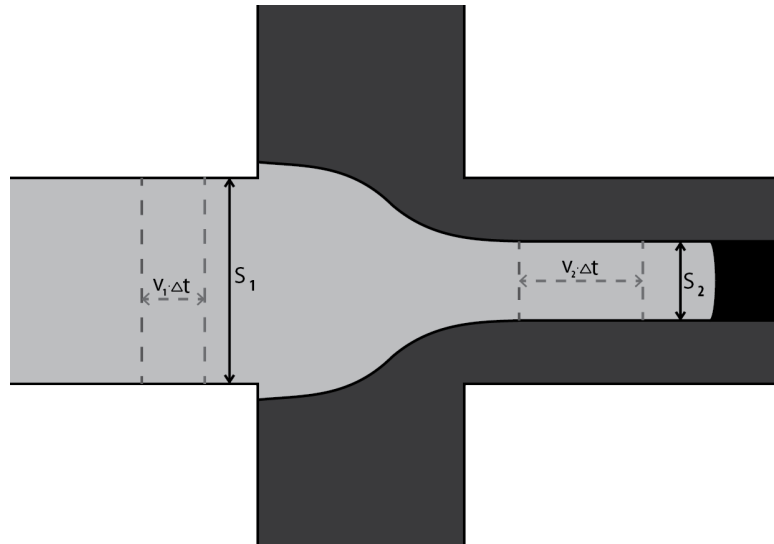


Figure 2.11. Schematic drawing of a shear driven SLB depicting change of speed in relation to channel width

The velocity of the SLB should in accordance with the expression above increase with the decrease of channel width (same flow over smaller area). This yields that:

$$v_2 = (S_1 \cdot v_1) / S_2 \quad (2.1)$$

3 Method

The descriptions of experimental preparations, SLB formation, driving an SLB with a shear force and formation of fibrinogen barriers are all based on an experimental setup using only one 6-way valve for switching. However, using this setup, air-bubbles sometimes found their way into the system during the many syringe changes, air-bubbles in the system destroys any formed SLBs. For this reason another setup using two 6-way valves was suggested by one of my supervisors, Peter Jönsson, that setup greatly reduced the risk of getting air-bubbles in the system as it was constructed in such a way that all tubings could be filled before any injection into the microfluidic channel. This new setup could be seen in figure 3.1 and a brief description of this setup and how it was used could be found in appendix C.

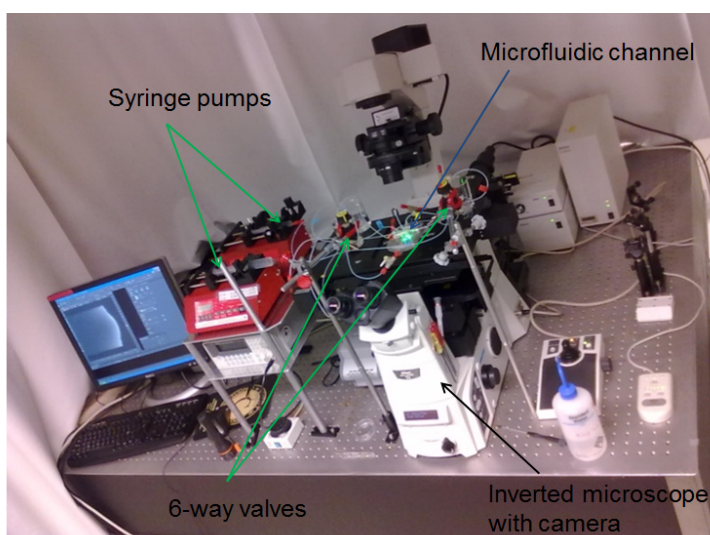


Figure 3.1. Experimental setup

3.1 Materials

1-palmitoyl-2-oleoyl-sn-glycero-3-phosphocholine (POPC) from Avanti Polar Lipids (Alabaster, AL) was used to form the bilayers and Lissamine rhodamine B 1,2-dihexadecanoyl-*sn*-glycero-3-phosphatidylethanolamine, $\lambda_{exc}/\lambda_{em.}=560/580$ nm) (R-DHPE) from Invitrogen (Carlsbad, CA) was used to label the SLB so that it became detectable in an inverted microscope Nikon Eclipse Ti-E microscope (Nikon Corporation, Tokyo, Japan) with an attached Andor iXon+ EMCCD camera (Andor Technology, Belfast, Northern Ireland) using a 60 \times magnification (NA = 1.49) oil immersion objective (Nikon Corporation). Glass substrates (0.13–0.16 mm in thickness, Menzel-Gläser, Braunschweig, Germany) were cleaned with TL1 cleaning solution (1 part ammonium hydroxide (NH₄OH), 1 part hydrogen peroxide (H₂O₂) and 5 parts MilliQ water). The microfluidic channels were replica moulded using polydimethylsiloxane (PDMS) formed from Sylgard 184 and curing agent (10:1 ratio) (Dow Corning, Midland, MI). The glass substrate and the PDMS were treated with plasma before they were bonded together (PDC-32G Plasma Cleaner, Harrick Plasma, Ithaca, NY).

For handling the flows and rates used in the microfluidic channel 6-way selection valves (Upchurch Scientific, Oak Harbor, WA) were used together with a syringe pumps (a NE-1000 and a NE-4000, New Era Pump Systems Inc., Wantagh, NY). Two different buffers were used during the experiments, the first will be referred to as buffer pH8 (100mM NaCl, 10mM Tris, 1 mM EDTA, diluted with HCL to pH 8.0) and the other buffer pH 5 (5mM NaCl, 2mM Tris, diluted with HCL to pH 5.0). A Kr-Ar mixed gas ion laser (Stabilite 2018, Spectra-Physics Lasers, Mountain View, CA) laser at 532 nm and 100 *mW* was used to bleach spots in the SLB during FRAP.

3.2 Fabricating microfluidic channels

The microfluidic channels used in this work are based on glass substrates on which replica molded polydimethylsiloxane (PDMS) with the structure of a microfluidic channel was irreversibly bound, see figure 3.2. The PDMS was then perforated from the top to allow access into the microfluidic reservoirs, after which silicone tubes were glued around each opening with the purpose to guide and secure connection tubings. For a more detailed description, see appendix A.

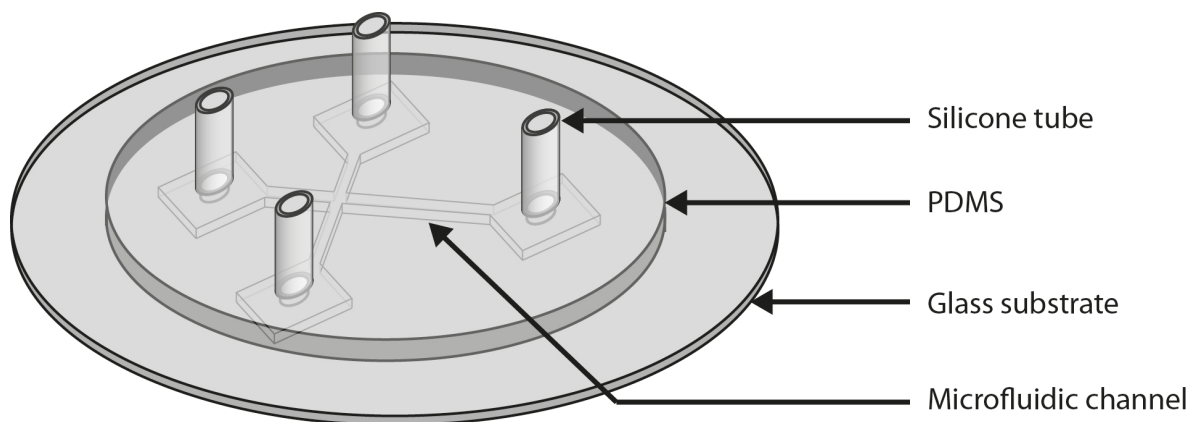


Figure 3.2. Sketch of a microfluidic channel

3.3 Preparation of lipid vesicles

In the experiments vesicles extruded through a 30 nm filter were formed with either a 0.1 or 1 wt% ratio of R-DHPE in relation to POPC lipids and diluted with buffer to a concentration of 1 mg/ml. A more detailed description is given in appendix B.

3.4 Flow regulation in the microfluidic system

The different steps involved in forming and driving an SLB requires a possibility to switch between different flows through different parts of the microfluidic channel. For this purpose a 6-way selection valve was used to regulate flows in and out of the different connections of the microfluidic channel. Each valve has a switch and six numbered connections, see figure 3.3. The valves have two modes, Inject or Load, figure 3.4 shows how these two modes combine different

connections with each other. Also the different steps in the experimental process require a precise regulation of the flow rates in the microfluidic system, this was provided by two syringe pumps, see figure 3.1.

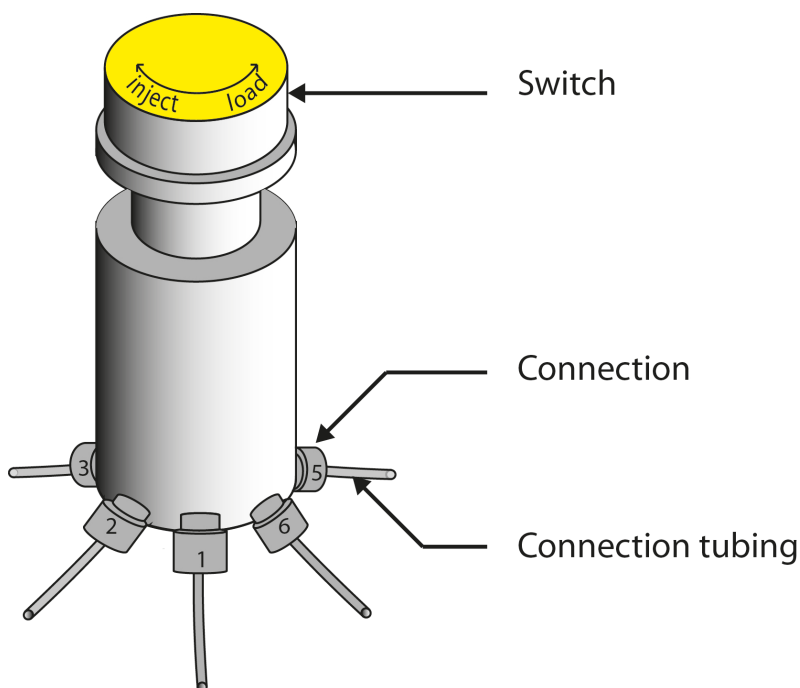


Figure 3.3. Sketch of a 6-way selection valve with numbered connections

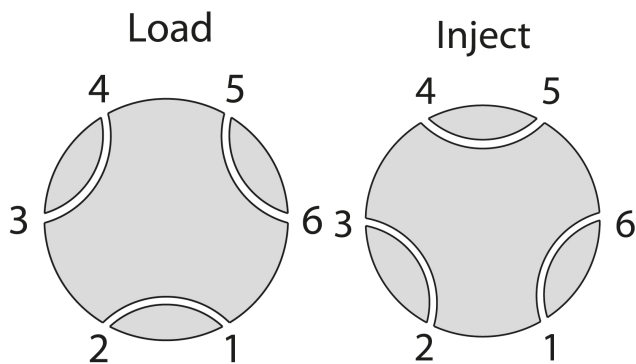


Figure 3.4. Schematic drawing of the two modes of the 6-way valves. The valve has two modes, Inject and Load, and in the figure it is shown how these different settings connect different openings with each other.

3.5 Experimental preparations

Before the experiments the microfluidic channels were sometimes cleaned with 2x200 μ l SDS 2 wt% back and forth through each inlet, then filled up with SDS and sonicated for about ten minutes. The channels were then rinsed with 2x200 μ l MilliQ through each inlet and filled with buffer pH8. Each channel was then checked for any trapped air bubbles, if found in the reservoirs or channel it was sonicated for about 2 minutes otherwise a pipette was used to remove bubbles. A microfluidic channel was then mounted in a custom made holder on the XY-table. The

microfluidic channel was placed in the holder; a Teflon ring was put on top. The channel was then adjusted so that it was straight – this was done using a 20x air objective together with using the Nikon software function intensity profile in order to place a crosshair. Once the channel had been aligned to this crosshair, three washers and bolts were used to secure channel position in the holder. Vesicle stock solution was also diluted to a concentration of 0.1 mg/ml 1 wt% R-DHPE in the buffer pH8.

The 6-way valve used in the experiments has two different settings shown in figure 3.4, it is either in Inject or in Load mode. A 20 ml syringe with buffer pH 8 was mounted in a syringe pump, with the 6-way valve set in mode Load tubing was connect to the syringe and purge was used on the syringe pump until no more air bubbles appeared at the end of the tubing connected to 5, then the 6-way valve was switched to Inject mode and purge was used until drops came from the tubing from connection 1. The syringe pump was set to pump at 20 $\mu\text{l}/\text{min}$, and tubing 1 was connected to the inlet on the microfluidic channel. A 5ml syringe with buffer was mounted into another syringe pump, tubings were connected and purge was used until no more airbubbles appeared, then the pump speed was set to 20 $\mu\text{l}/\text{min}$ and connected to inlet 4 on the microfluidic channel (figure 3.5).

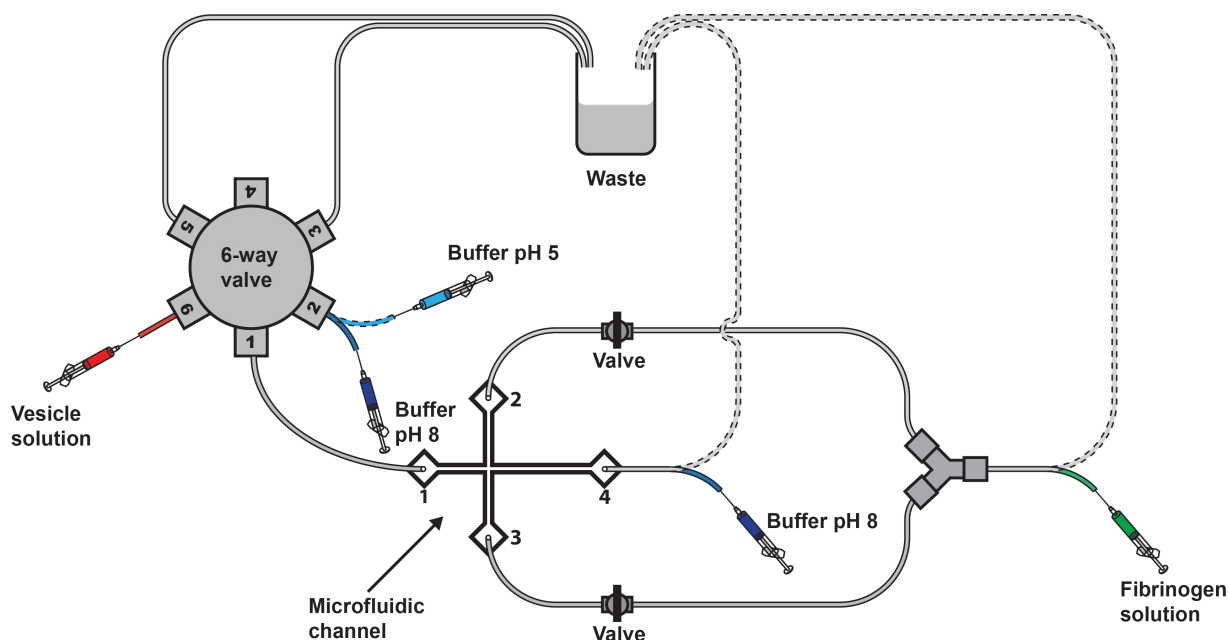


Figure 3.5 Schematic drawing of the basic setup (top view, not drawn to scale).

Tubings were mounted to inlet 2 and 3 on the microfluidic channel, with their other ends ending up in a waste jar. The microfluidic channel was typically rinsed for about five minutes. After this the 20 ml syringe pump was turned off and the connection was put into waste.

3.6 Forming a bilayer in a microfluidic channel

When forming an SLB in the microfluidic channel a syringe with 0.4ml vesicle solution was mounted in a syringe pump and connected to connection 2 on the 6-way valve (purge was used until no more air bubbles came from 3), the flow rate was set to 20 $\mu\text{l}/\text{min}$ and the 6-way valve switched to load. Vesicle solution was then injected into the microfluidic channel for about 10 minutes, or until an SLB had properly formed (figure 3.6.B). The syringe pump with vesicle solution was stopped and the 6-way valve switched to inject, the connection was then put into waste, the 6-way valve switched to load. A 20 ml buffer was connected with the pump speed set to 130 $\mu\text{l}/\text{min}$ until droplets came from connection 2, then the speed was changed to 30 $\mu\text{l}/\text{min}$ and the 6-way valve switched to inject and the microfluidic channel was allowed to rinse for about 10 minutes.

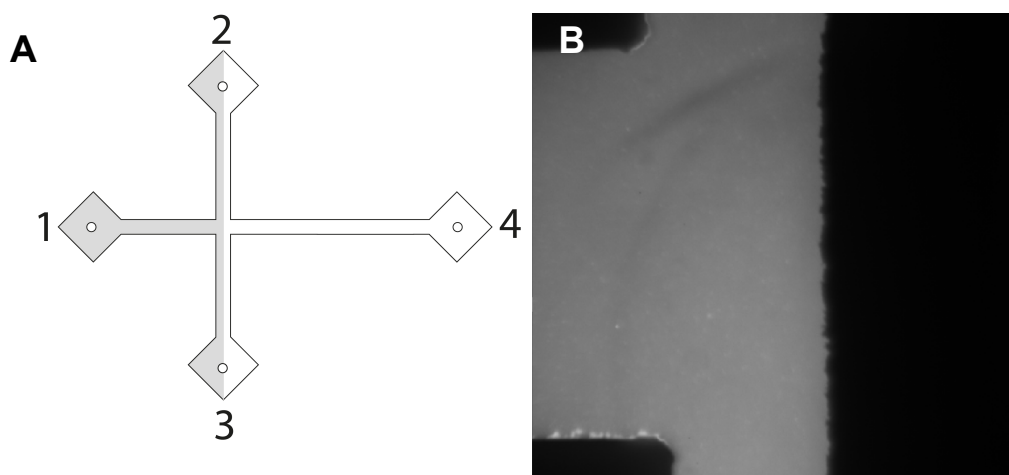


Figure 3.6. (A) A Schematic drawing of the microfluidic channel with a formed SLB (top view, not to scale) (B) A formed SLB in a microfluidic channel

3.6.1 Driving an SLB with a shear force

After the bilayer had been formed it could be driven with a shear-force as described earlier. The 5ml buffer was disconnected and the connection was put in waste, the valves on connection 2 & 3 were closed and the 20 ml buffer flow rate was increased to 200 $\mu\text{l}/\text{min}$, see figure 3.7.

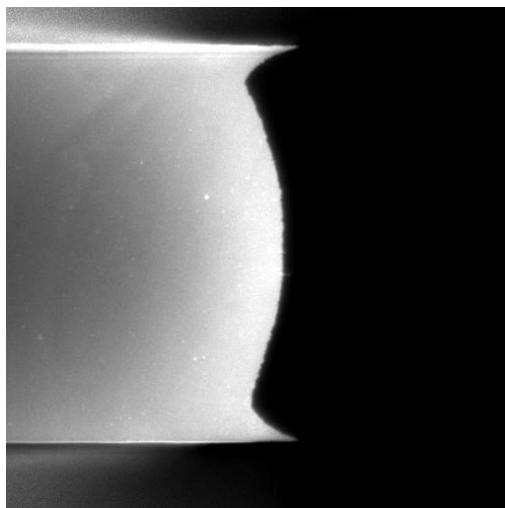


Figure 3.7. Driving the SLB with a 200 $\mu\text{l}/\text{min}$ flow

A separation of accumulated molecules at the front could then be performed by reversing the flow in the channel. This could be achieved by disconnecting the 20 ml buffer and putting connection into waste, then reconnecting the 5 ml buffer (be sure to have droplets both on syringe and connection in order to prevent any air to enter the system) and set the flow rate to 200 $\mu\text{l}/\text{min}$.

3.7 Forming fibrinogen barriers in a microfluidic channel

In order to maximize fibrinogen adsorption on the substrate, a buffer solution was used with low ion content 5 mM NaCl and 2 mM TRIS at pH 5.00[28]. Two syringes were mounted in a syringe pump, each with 100 μl fibrinogen solution (1 mg/ml) diluted with 900 μl buffer. The syringes were then connected to inlet 2 and 3 respectively. A 20 ml syringe filled with the low ion content and low pH buffer was mounted in another syringe pump and connect to inlet 1 on the microfluidic channel. The buffer solution was injected at 50 $\mu\text{l}/\text{min}$, while the fibrinogen solution was injected with 10 $\mu\text{l}/\text{min}$, see figure 3.8. This injection ratio between buffer and fibrinogen solution will in the rest of the text be referred to as 5:1:1. To ensure sufficient adsorption the injection continued for about 60 minutes, and then the fibrinogen was stopped and inlets 2 and 3 switched with a 6-way valve to work as outlets while the buffer was used at the same injection speed to rinse the channel for about 30 minutes. In some of the experiments another injection

ratio was used with 40 $\mu\text{l}/\text{min}$ buffer flow and 20 $\mu\text{l}/\text{min}$ for the fibrinogen solutions respectively, this ratio will later be referred to as 4:2:2.

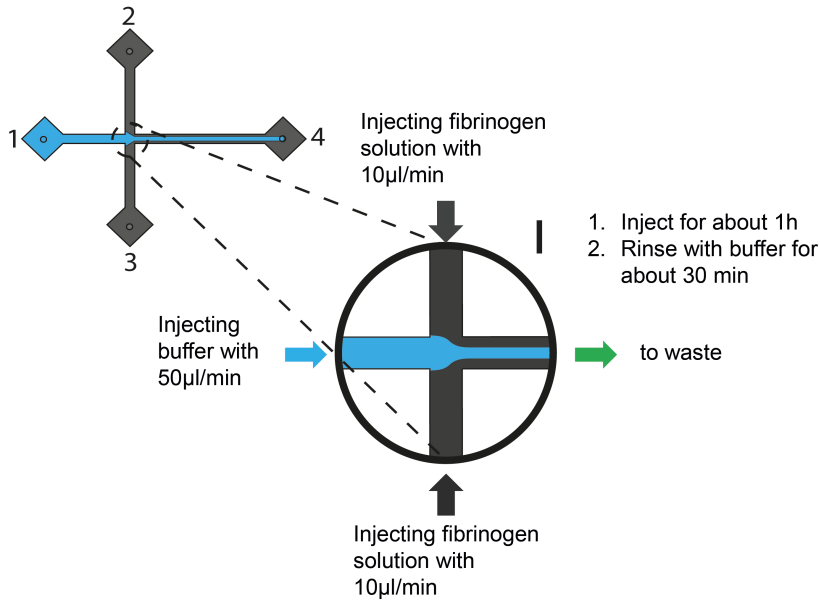


Figure. 3.8 Schematic drawing of the microfluidic channel (top view, not to scale) depicting the steps involved in fibrinogen barrier formation

3.8 Inverted microscope and camera

Light from a mercury lamp is filtered through an excitation filter which only lets through wavelengths suitable for rhodamine excitation, see figure 3.9. This light is then reflected by a dichroic mirror (reflects light from a certain direction and lets through light from another), and focused through an objective onto the substrate surface. At the enlightened area at the substrate surface, some photons encounter the fluorescent molecules in the sample and excite them while other light is scattered in all directions. Upon returning to their original state the excited fluorescent molecules emits light in all directions of longer wavelengths compared to the ones needed for excitation. Some light finds its way down through the objective and through an emission filter which only lets through the wavelengths emitted by the fluorophore.

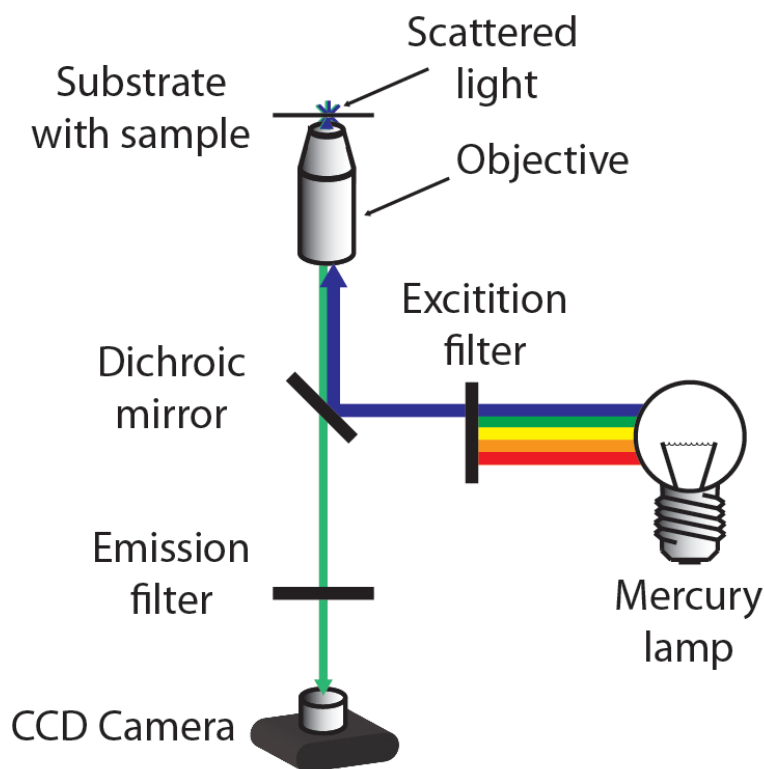


Figure 3.9. Sketch of the epifluorescence microscope setup

3.9 Fluorescence Recovery After Photobleaching (FRAP)

The Fluorescence Recovery After Photobleaching (FRAP) method was used in this work to determine diffusivity of lipid molecules in a formed SLB. FRAP utilizes the light emitting property of fluorescently tagged molecules. Assuming that the molecules are uniformly spread on a surface and by exposing a small area of the surface to high intensive light in the form of a laser this will result in a darkened spot. The reason for this is that the fluorescent molecules in the exposed area are damaged by photochemical reactions and do no longer fluoresce and therefore turn dark. Based on natural lipid diffusivity within the SLB, the bleached lipids will start to migrate out of the bleached area, while other unbleached lipids will migrate into it. Thus, after some time, the lipids will have mixed so much so that no trace is left of the previously bleached spot. A camera was used to take images of the SLB surface at a certain interval; it started taking pictures before the bleach and continued for about 90s after. The images were then saved as a stack and imported into MATLAB, where the diffusivity was determined using the Hankel transform method [31].

4 Results & Discussion

Many hours of experimentation was conducted with varying degrees of success as the experiment were rather complex regarding the amount of implementation steps and due to the uncertainty of surface conditions determining SLB formation as well as other key properties. It was found that the most critical aspect of these kinds of experiment was to ensure proper surface conditions so that an SLB would actually form and so that the SLB would not encounter any impurities on the surface which tend to affect experimental outcomes. This was problem was not satisfyingly solved during this work and has to be further investigated. Although a good channel once found used only with SLBs could be satisfactory cleaned with SDS and reused a couple of times, there are no similar methods to use to remove fibrinogen. Channels were cleaned with 2 wt% deconnex in a similar fashion compared to SDS the cleaning described in this work although they were left in the sonicator for about 30 minutes. An experiment on one such cleaned channel showed that there was still some fragments of fibrinogen left in the channel which had not been removed. It might still be possible to reuse these channels in experiments where new fibrinogen barriers are formed as the observed fibrinogen fragments were situated in regions where there had been barriers previously and close to the walls.

The first results presented here deals with different aspects of fibrinogen barrier and then there is a comparison over differences in SLB front velocity and accumulation of fluorescent molecules for the cases of driving an SLB in a channel with or without fibrinogen barriers.

4.1 Properties of the fibrinogen barrier

It has shown that forming a sufficiently strong fibrinogen barrier is non-trivial. Fibrinogen adsorption to the surface depend on a range of factors such as concentration, flow rate, time, pH and ion concentration of buffer used to dilute fibrinogen[28]. In many experiments, where these factors hadn't been optimized, the fibrinogen barrier has shown burst under the pressure on it from the moving SLB. Also fibrinogen aggregates over time, leading to a reduced net concentration of unaggregated fibrinogen in stock solution. To get an idea of how much of the fibrinogen had aggregated, three different samples were prepared. Buffer was first filtrated through a 22 nm filter and then used as a control, it was also used to dilute first a fibrinogen stock solution that had been kept in the refrigerator for many weeks and then for a freshly made stock solution. Both stock solutions used an outdated fibrinogen batch. These samples were then studied with the nanosight tool; the different concentrations of different sized aggregates are shown in figure 4.1. The mean size of the aggregates in the newly made stock solution from the old batch was 160 ± 72 nm, and for the old stock solution from the old batch was 212 ± 81 nm. This indicates that the fibrinogen proteins do aggregate over time. So, when making a stock solution it might not necessarily contain the expected concentration of unaggregated fibrinogen, although it might be possible to do an approximation based on measurements with the nanosight tool. It is

unclear how these aggregates adsorb to the channel surface, but it has been observed in experiments using fibrinogen solutions with more aggregates, that the fibrinogen barriers does not form as densely compared to cases with less aggregates. The size of fibrinogen during crystallography as mentioned before was ~ 7 nm width and ~ 45 nm length, however in solution the protein folds and the folded fibrinogen is likely to have a diameter less than 30 nm, which is the minimum threshold size that nanosight can detect. This would explain why there is no distinct peak describing the unaggregated fibrinogen in the figure.

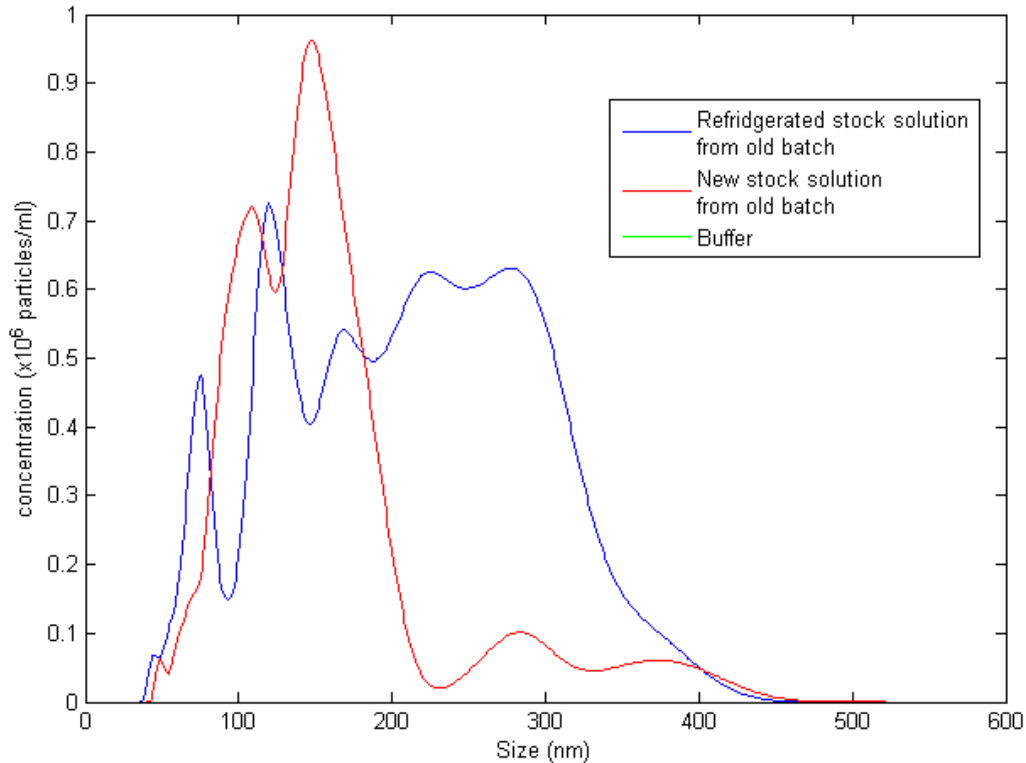


Figure 4.1. Distribution of concentrations of fibrinogen aggregates in 1 ml samples.

For this reason a higher concentration was used to be sure to exceed the limit of the fibrinogen concentration where adsorption increases (~ 50 $\mu\text{g/ml}$). Having said this, during several experiments, the fibrinogen barrier, at exaggerated concentrations and under optimized conditions, was shown to be sufficiently strong. A majority of the experiments were made with an old batch of fibrinogen where the best before date had been passed. A new fibrinogen batch arrived first at the end and it would be interesting to check the aggregation ratio with the nanosight tool in a similar experiment.

Fibrinogen stock solution is said by the manufacturer to hold for a week in the refrigerator and one way of optimizing fibrinogen adsorption with regard to concentration could be to dilute the stock solution with buffer to samples of different concentration after which the optimal concentration for fibrinogen adsorption could be determined with QCM. After this the stock

solution could be made into many samples of this optimal concentration and put in the freezer as this would probably greatly reduce the rate of aggregation. A sample could be unfrozen and analyzed with QCM to be compared with the adsorption of the previous sample that was checked directly from the refrigerated stock solution, to ensure that the freezing process does not affect adsorption.

As could be seen in figure 4.2B very few vesicles adsorb unto surface were a fibrinogen barrier has been formed, vesicles could probably just adsorb where no fibrinogen has adsorbed prior, therefore as vesicles are injected they adsorb within the constraints of the fibrinogen barrier.

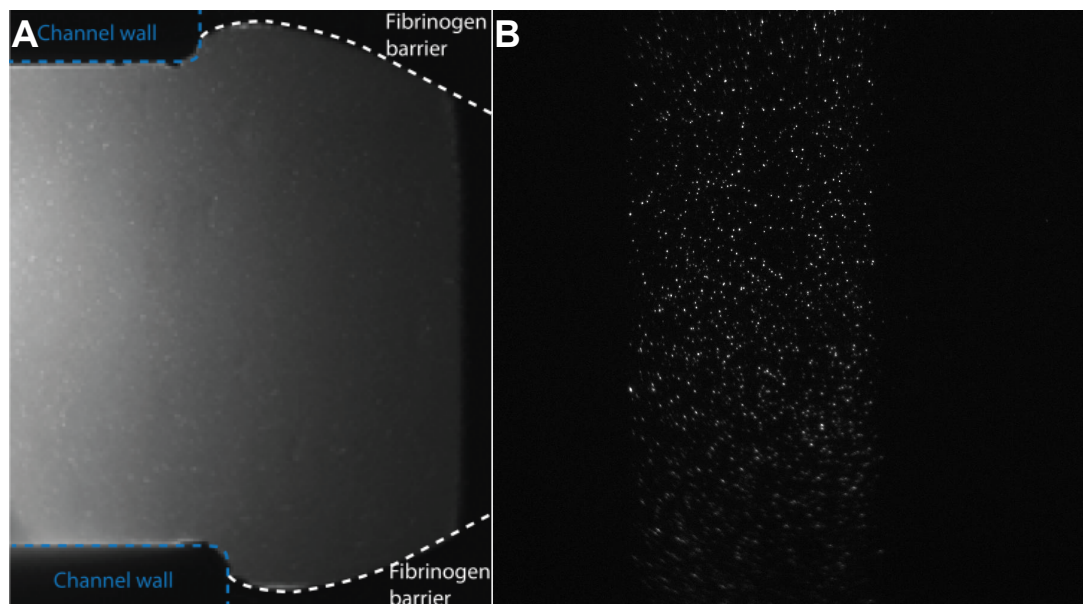


Figure 4.2. (A) SLB formed in cross channel with fibrinogen barriers formed prior (B) Very low vesicle adsorption in the fibrinogen barrier in side arm

It was observed that when fibrinogen adsorption is not dense enough, a shear driven SLB is able to push the barrier back, see figure 4.3.A. It has also been observed that there is a peculiar loss of accumulated fluorescently labeled lipids that occurs in small patches when the fibrinogen barriers give way completely or just partly which manifest itself by the channel in between obtaining a rugged edge as the SLB progresses, see figure 4.4.B.

Figure 4.3. (A) When a fibrinogen barrier has not formed densely enough it cannot withstand the pressure exerted on it by the shear driven SLB as it is driven with a 200 $\mu\text{l}/\text{min}$ flow (B) The fibrinogen barrier holds well during a 200 $\mu\text{l}/\text{min}$ push when the fibrinogen has adsorbed densely enough.

In other experiments where buffers were switched during a push from pH 8 and high ion content to a buffer with pH 5 and low buffer content and back again, it has been observed that part of the bilayer front during the change can pass down into the lower sheet of the bilayer or possibly unto the surface of the channel where they get stuck under the advancing SLB. This has been seen to manifest as a stationary light grey copy of the SLB front profile. It would seem that the fluorescent molecules stuck under the SLB makes it stick up a bit as fluorophores in the top layer in most cases are seen to accumulate over them. Typically, the diffusion of the molecules that are

trapped under the SLB is remarkably slow and a long time experiment showed that the greyish profile remain for a long time (>1 h) after the bulk flow is stopped. So, trying to link the two observations together, under some conditions it may be possible for some of the accumulated molecules to follow the bilayer down into the lower sheet and it might be that when the SLB front with an accumulation of molecules encounters fibrinogen barrier that could be unevenly pushed back, in the interaction process, some of the accumulated molecules do follow the rolling motion down into the lower layer. Also an ordinary accumulation has been observed at the sites of these light greyish profiles which would only be the natural case as the SLB would curve itself slightly where it is moving over the accumulation in the lower sheet.

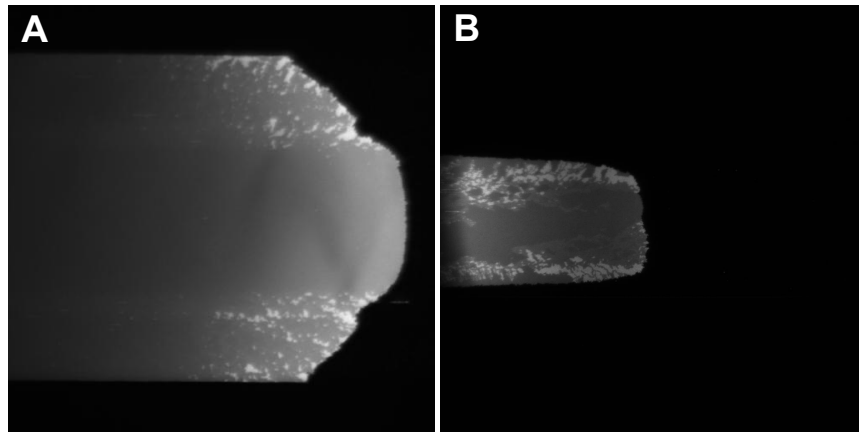


Figure 4.4 (A) Rhodamine clogging in the areas where the fibrinogen barrier has been pushed back (B) A lot of Rhodamine clogging although fibrinogen barrier intact but a bit spiky.

4.1.1 Effects of diffusion on fibrinogen barrier formation

During fibrinogen barrier formation, there is a constant diffusion between the injected fibrinogen solution and the buffer, meaning that more and more fibrinogen will diffuse over into the buffer solution area and an increasing number will adsorb to the surface with increasing distance. Also important is the time of injection as the distance between the fibrinogen barriers will decrease with increasing injection time; this has to be contrasted with the need of forming a solid fibrinogen barrier in the area of interest.

From experiments, the initial change in distance between the fibrinogen barriers measured at a point $50\text{ }\mu\text{m}$ behind the SLB front over a $119.3\text{ }\mu\text{m}$ distance is measured to be $1.9\text{ }\mu\text{m}$, see figure 4.5.A. This would be a reasonable approximation of the actual change in solid channel width over distance. A reason why this could work as approximation is that the diffusion profile during fibrinogen barrier formation will look the same, it will only move towards the center of channel over distance, so there will be an equal amount of soft barrier to push back at every time instant. Something that might be relevant though is that the ratio between soft barrier to push back and SLB width will change over distance.

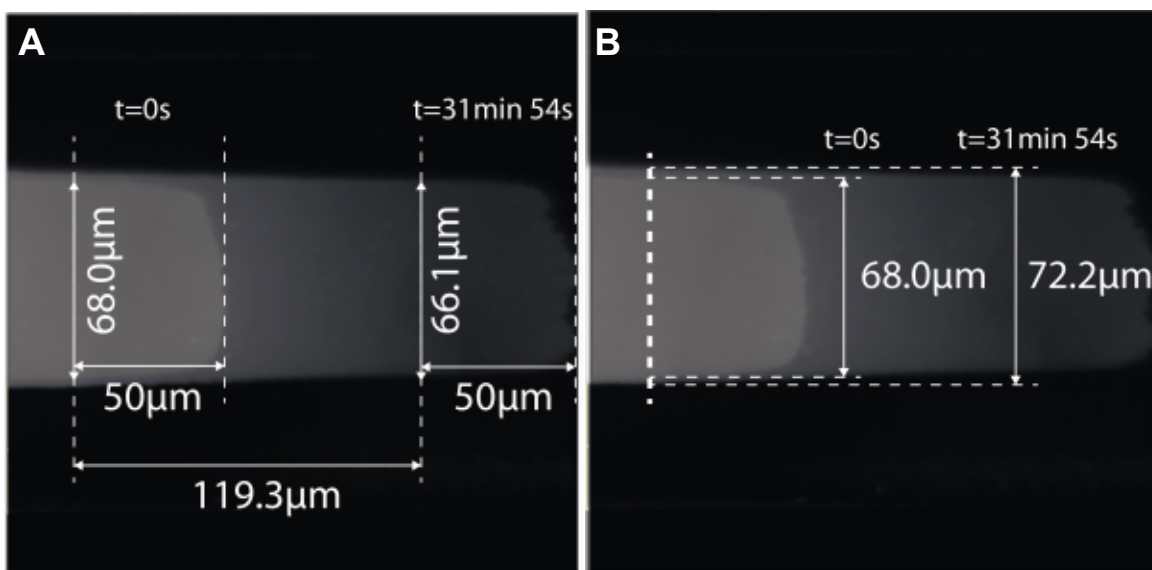


Figure 4.5. (A) An overlay of the advancing SLB at two different times, showing the channel width $50\mu\text{m}$ behind the SLB front at each time (B) Channel width at a certain point in time compared to channel width at same location 31min and 59s later, an increase is observed.

Further it was observed that the channel got pushed back by the advancing SLB with time as the channel that was $68.0\mu\text{m}$ wide at a certain point in time was measured to be $72.2\mu\text{m}$ wide after an additional 31 minutes and 59 seconds, see figure 3.4.B. Analyzing this increase in width further for another case, it showed that the increase was greatest just as the SLB front was passing a certain point and then the widening stabilized over time, see figure 4.6. The resulting widening of the channel for this case came to about $7.1\mu\text{m}$, this could be compared with the result of a study for another experiment where the widening stabilized at $7.0\mu\text{m}$. It is interesting to notice that the widening was almost similar in both cases although for the first case the starting channel width was $74.3\mu\text{m}$ and for the other case $64.1\mu\text{m}$.

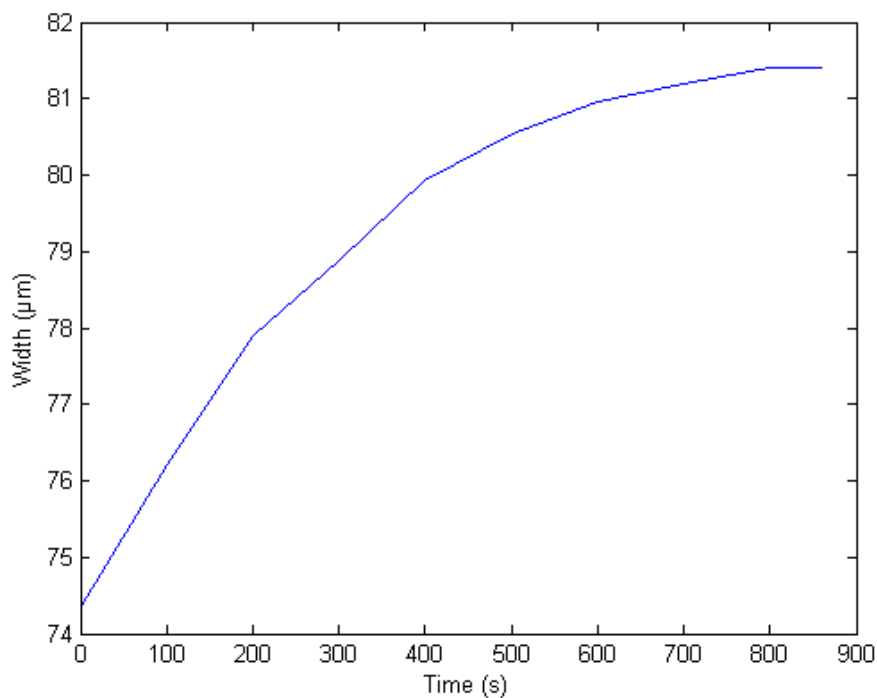


Figure 4.6. Increase in distance between fibrinogen as a function of time. First measurement taken 19.38 μm behind SLB front.

The constant diffusion between the fibrinogen and the buffer during fibrinogen barrier formation makes the channel become narrower with increasing distance. This means that the diffused fibrinogen might not have formed a very solid barrier in the diffusion region. So, in the diffusion region of the formed barrier the fibrinogen has not adsorbed as densely as further into the barrier region, this makes, as in the case previously mentioned, for a barrier that can be pushed back by the moving SLB. Some of the force driving the bilayer is therefore lost as it is used to push the not so solid barrier back.

4.1.2 Fibrinogen might bind to an SLB

Several consecutive measurements showed that when fibrinogen was injected after the bilayer was formed and pushed for about 1h, fibrinogen seem to bind to the SLB and accumulate at the SLB front instead of the fluorescently labeled lipids, see figure 4.7. If fibrinogen could bind to SLBs, then it is unclear how the fibrinogen binds to the SLB, if it only adsorbs on top of it or if it is actually incorporated into one or both of the two layers. During SLB formation some vesicles could be seen to adsorb to the SLB after the bilayer has formed, they typically stick to the SLB but can move along it with the bulk flow.

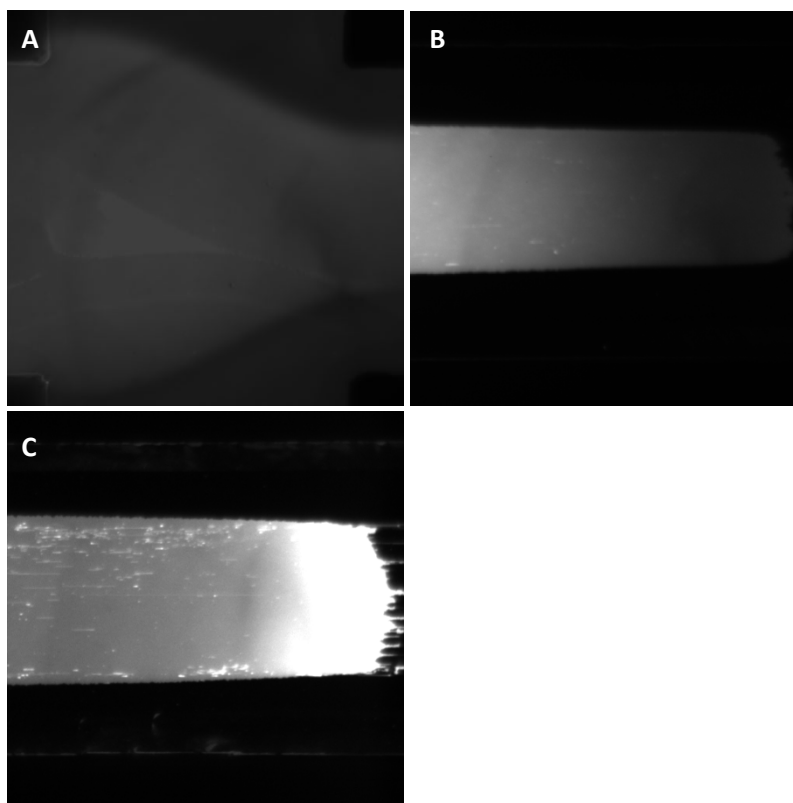


Figure 4.7. (A) Fibrinogen injected after an SLB had been formed and pushed for ~1h or more (B) Possible accumulation of molecules which are not fluorescently labeled at the SLB front (C) Accumulation of fluorescently labeled lipids in a channel where the fibrinogen barrier was formed prior to SLB formation

In a previously published case it has been seen that different membrane bound molecules mix with each other at the front of the SLB [6]. Therefore it could be assumed that both incorporated molecules would accumulate equally much at the front, but that would then show as a weaker accumulation compared to the case when no fibrinogen has bound into the SLB as the fibrinogen is fluorescently unlabeled. Instead it would seem that fibrinogen and fluorescently labeled lipids compete in such a way that fluorescently labeled lipids are pushed away from the SLB front further back in the SLB as fibrinogen is accumulating. Another possible explanation would be

that fibrinogen molecules somehow finds its way to and deposits in front of the bilayer, where they are encircled by the moving SLB. Many such encircled fibrinogen molecules could then act as an array of nanosized filters, filtering out the larger fluorescently labeled molecules. FRAP was performed after fibrinogen barriers had been formed and after the SLB had been driven with a shear-force for about an hour. The first one was done in the area where fibrinogen solution had passed for about 30 minutes time during fibrinogen barrier formation, it was analyzed with the Hankel transform[31] and the diffusivity was determined to be $D_1=2.23 \mu\text{m}^2/\text{s}$. A similar analysis was performed in an area in the middle of the channel where only buffer had passed and the diffusivity there was found to be $D_2=2.09 \mu\text{m}^2/\text{s}$. The difference in diffusivity is non-significant, and if fibrinogen had penetrated the SLB in areas where it had passed and adsorbed to the surface and immobilized there, then the diffusivity there would be lower and not higher as was the outcome of the FRAP analysis. Another experiment which could be performed to determine what happens would be to do measurements with quartz crystal microbalance (QCM) on an SLB formed on a crystal after which fibrinogen could be introduced in the bulk solution. If the fibrinogen in any way adsorb to the SLB it would show as a frequency shift of the crystal.

4.2 Comparisons of driving a bilayer with or without a fibrinogen barrier

4.2.1 Velocity of SLB front

For one batch of vesicles the velocity of the front of an SLB, driven with a $200 \mu\text{l}/\text{min}$ flow, was found to be $0.125 \pm 0.03 \mu\text{m}/\text{s}$ for three different experiments under similar conditions. A reference value given in literature for the same flow speed is $\sim 0.2 \mu\text{m}/\text{s}$ [5], which clearly differs from the results obtained in several consecutive experiments using different batches of microfluidic channels. But, it would show that for a new batch of vesicle stock solution the velocity for the same case was $0.23 \mu\text{m}/\text{s}$, which is more in agreement with the literature value. This would suggest that the velocity of a shear-driven SLB is sensitive to some unknown element in the vesicle batch preparation. Now, only three batches were used within this work, but their quality all seem to affect the velocity even if there was a better agreement in velocity between SLBs formed from the first and last batch. It might be that since the results of the second batch differs so much in comparison to what is reported in literature, that not all of the methanol was successfully evaporated from the vesicle batch during the manufacturing process.

Different bulk flows Q were used during the experiments; therefore it is convenient to represent the normalized velocities v/Q , where v is the measured velocity in m/s . The reason that this is convenient is that SLB velocity scales linearly with the bulk flow rate [5], which makes the measured values at different bulk flows comparable, see table 4.1.

	Number of experiments	Vesicle batch 1	Vesicle batch 2	Vesicle batch 3	Reference value[5]
No fibrinogen v/Q (m^{-2})	3		38±1		62±3
	6			70	
	1				
5:1:1 fibrinogen v/Q (m^{-2})	1		52		
4:2:2 fibrinogen v/Q (m^{-2})	1	80			

Table 4.1 SLB front speed

The surface conditions of manufactured channels varied a lot, but this had more effect on bilayer formation than on the SLB front velocity. This could be seen in table 3.1 where the velocity is surprisingly consistent although the surface properties were really different for some of the cases.

Since different vesicle batches were used and this seem coupled to the velocity of the SLB, it would seem more appropriate to present difference in velocity with or without a fibrinogen barrier as a ratio. SLB front velocity increased with 36% when driven inside a channel with 5:1:1 fibrinogen barriers.

In the case where the fibrinogen barrier was formed after the SLB and the SLB had been pushed, assuming that the fibrinogen adsorbed onto the bilayer, there was a slow deceleration of the moving SLB noticed in relation with increasing amount of accumulated fibrinogen at the front.

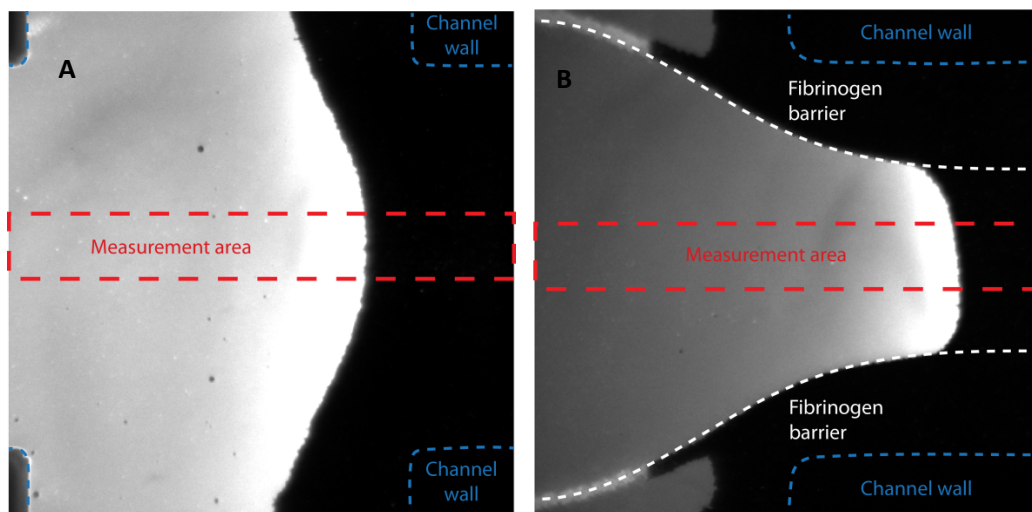
Calculating the change in SLB front velocity using equation 2.1 gives that the velocity in the 5:1:1 channel should be 0.248 $\mu m/s$, based on a measured SLB front velocity of 0.123 $\mu m/s$. This could be compared to the measured velocity with a fibrinogen barrier of 0.174 $\mu m/s$. Width between fibrinogen barriers were measured at a point 26.22 μm behind the SLB front for two cases, and the average width was used as S_2 in the calculations. The measured velocity was determined from SLB front positions of these two cases, which gives an average velocity over the distance. The discrepancy between calculated and measured increase in SLB front velocity could possibly be explained by the observed expansion of the SLB in other directions than forward and also some of the force driving the bilayer forward is lost pushing back the fibrinogen barrier. Another reason for the discrepancy might be that the SLB front velocity is measured at a point in the channel center and is assumed in the calculations to be equal across the channel width while it in reality is higher in the center of channel.

Another way of comparing this difference in velocity which was not carried out in this work, would have been to measure the velocity using FRAP of the SLB at a point before the cross in the channel and compare it with a measurement using FRAP of the velocity at a point within the narrower channel in the fibrinogen.

4.2.2 Accumulation of fluorescently labeled lipids

One of the main purposes of using fibrinogen barriers was to achieve a more efficient accumulation of incorporated molecules at the SLB front. A way to determine how accumulation profiles differ between an SLB being driven in a channel with or without fibrinogen barriers is to study intensity plots. An intensity plot is a plot of intensity values along a line through the SLB to be studied. In the cases shown in figure 4.8.A-B however, multiple lines from a selected area are averaged against each other in order to avoid any local extremes that could occur. The profile thus obtained is much smoother in comparison to a single line profile. As the illumination in the microscope is uneven, for each case, three samples of the background far from the SLB front were taken and combined into a median image using imageJ, and all images were then divided by the median image of respective case. Furthermore the median of non-zero intensity values of spots in the images that should be black were subtracted from all intensity values in all images. Also, median values were taken of the SLB for each case in areas without fluorescence accumulation; all images were then normalized with this value, thus giving SLBs without accumulation an intensity value of one.

With normalized images, three intensity profiles with a 120 s interval have been plotted for both cases as could be seen in figure 4.8.C. Images were compared for the two cases which were taken at approximately the same time after they begin to move under an increase in bulk flow to 200 $\mu\text{l}/\text{min}$. The case without fibrinogen is marked with blue and the one with is marked with red. Figure 3.8 shows a faster accumulation of fluorescently labeled lipids in the case with fibrinogen barriers in comparison to the case without. An indication of an increase in velocity of the SLB front in the case with fibrinogen in comparison to the one without could be seen as the peaks get noticeably unaligned over time.



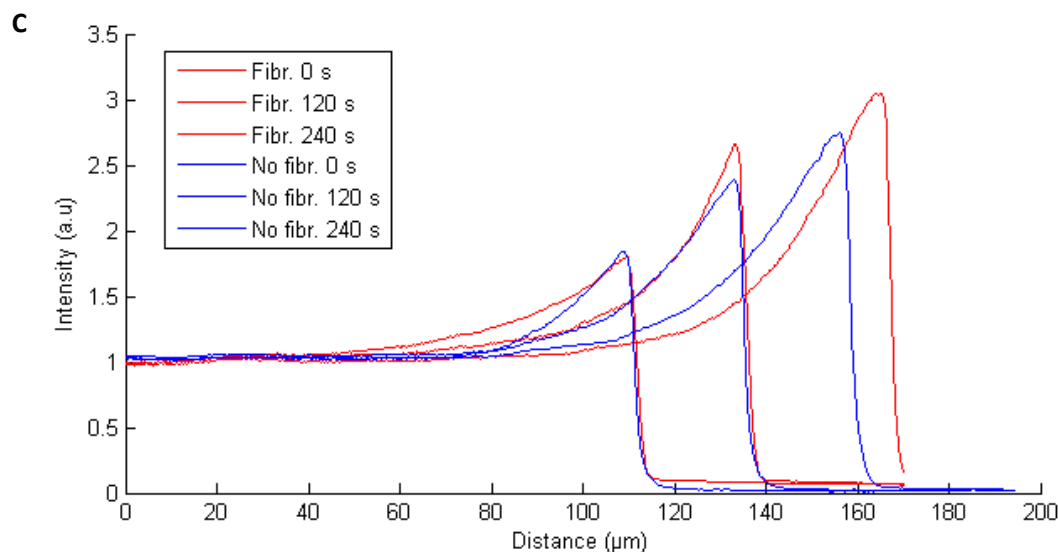


Figure 4.8. (A) SLB driven with a 200 $\mu\text{l}/\text{min}$ bulk flow in a channel without fibrinogen barriers. (B) SLB driven with a 200 $\mu\text{l}/\text{min}$ bulk flow in a channel with fibrinogen barriers. (C) Intensity profiles plotted for both cases with 120 s interval.

Intensity peak values were plotted at 20 s interval for the same cases shown in figure 3.8 during four minutes after the SLBs started moving, see figure 4.9. In the case with fibrinogen barrier, it remains solid for only the first four minutes after which it starts to break. However, during these four first minutes a difference in accumulation efficiency over time could be seen. It would seem that there is a steady, close to linear increase in fluorescence accumulation for the case with fibrinogen barriers, while for the case without fibrinogen the increase seems to be slightly curved or at least slower. Further experiments needs to be made where the fibrinogen barrier stays intact in order to determine long term differences in fluorescence accumulation between the two cases.

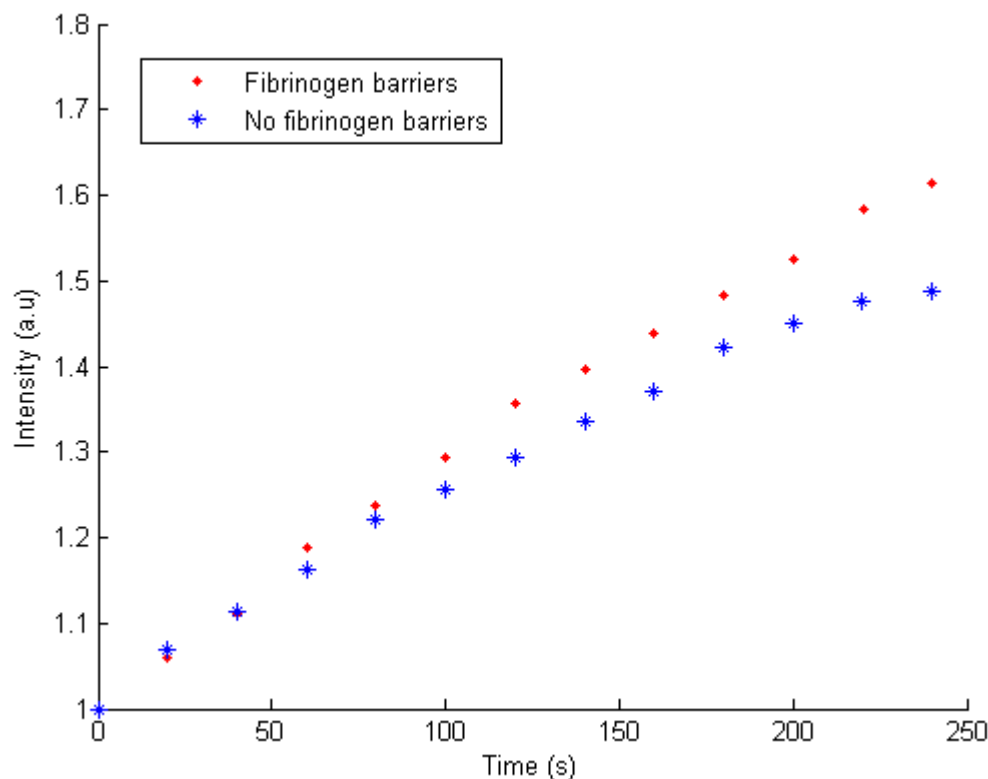


Figure 4.9. Increase in accumulation peak values over time for the case with and without fibrinogen barriers.

For cases without fibrinogen, it was noticed for longer runs that intensity peak values reached a certain level after which no increase was noticed. Although, these peak values differed between the different cases and also the times it took to stabilize. An explanation might be that different surface conditions and different hydrophilicity of the PDMS walls might affect how much the SLB spreads up onto the walls, a spreading unto the walls could be seen as an uncontrolled broadening of the channel. It is shown in [6], that the velocity is highest at the center of channel, leading to that fluorescent lipids accumulate faster there after which they spread out towards the sides of the channel. Once the accumulated fluorophores have reached the sides of the channel, the velocity there is close to zero meaning that they will remain there until they have dispersed through diffusion. This phenomena can be seen in figure 4.10.A, this is the reason why the accumulation peak values of SLBs in channels without fibrinogen barriers seem to stabilize at some level, the accumulation reaches an equilibrium at which as many fluorescently labeled lipids arrive at the front in comparison to the ones lost to the sides of the channel. It could be further observed, for the case with fibrinogen barriers, both that the SLB front is much flatter and that the accumulation profile at the center of the channel is very similar to one close to one of the barriers, see figure 4.10.B. The reason for this is that the flow profile is more even in the region to which the SLB is restricted by the fibrinogen barriers. Fibrinogen barriers thus mean that the loss of fluorescently labeled lipids is reduced, both unto the sides of the channel and unto the

walls. This reasoning further suggest that there might not be any stabilization at a certain peak value over a very long time for the case with fibrinogen barriers, something that needs to be verified by future experiment. If this really is the case, this would mean a possibility to accumulate SLB incorporated molecules to very high concentrations. This would be beneficial both for the purpose of measurement, giving a stronger signal, and for the case of separation, ensuring better separation as well as allowing for higher concentrations of separated molecules.

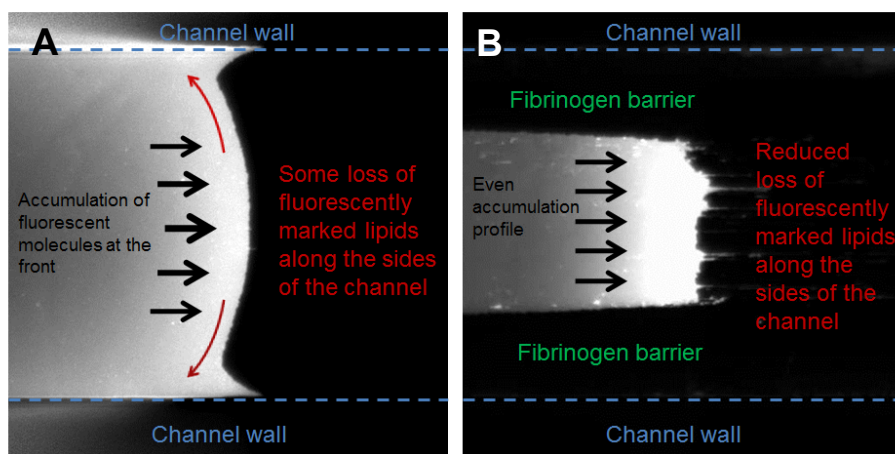


Figure 4.10. (A) Accumulation profile during SLB push at 200 $\mu\text{l}/\text{min}$ without fibrinogen barrier. (B) Accumulation profile during SLB push at 200 $\mu\text{l}/\text{min}$

5 Conclusion and Outlook

Many experiments were made with varying degree of success, and also the recording of data was not always done as would have been preferred in hindsight. The majority of the observations in this report were seen in many experiments, but some of the findings are only based on a limited number of recorded measurements and needs to be further verified. Also, some hypotheses are made for which some experiments are suggested which could help to determine their validity.

It was observed during this work that the fibrinogen barriers needed to be optimized in order not to lose accumulated material. Sufficient optimization was achieved in some of the experiments where the fibrinogen barriers did not burst even after a long time ($> \sim 1$ h). A suggestion for a working method to ensure sufficient fibrinogen barrier formation is described in the thesis. Even with a sufficient fibrinogen formation there is a diffusion region in which the fibrinogen adsorption is not so dense, this meant that the advancing SLB was able to push back the fibrinogen barriers. This widening of the channel was seen to settle about 7 μm for some different cases. This widening did not result in any loss of accumulated material. Also, the diffusion increase over distance resulting in a channel that narrows over distance, which was confirmed in the experiments. The narrowing depends on the square root of the time it takes the fibrinogen to pass through the channel, the angle at which the channel gets more narrow decrease over time.

An expected increase in SLB front velocity was observed although not as high as in theoretical predictions, one reason for this could be that the SLB travelled both forward but also towards the side as the channel widened also the SLB front velocity in the calculation is assumed to be same across the channel, while it in reality is higher in the center of channel.

A comparison was made of accumulation efficiency when the SLBs first start to move for cases with and without fibrinogen. It showed that even during the first four minutes of SLB motion, there is a noticeable difference where the case with fibrinogen shows a more efficient accumulation. This was the anticipated result as the constriction of the SLB by the barriers means that the SLB cannot spread unto the walls of the channel and also that the SLB is kept in the middle region of the channel where bulk flow differences are much smaller, this was observed as the SLB front was noticeably more flat in the case of fibrinogen barriers. For the case without barriers, accumulated molecules are constantly moving from the center of the SLB front out towards the sides where they remain and start to diffuse while center of the SLB front keeps moving forward, eventually equilibrium is reached when the same number of molecules are accumulated in comparison to the number lost. This hypothesis has been confirmed in observations during this work but nothing conclusive could be said as the level at which stabilization occurred differed from case to case, assumingly dependent on surface conditions and the hydrophilicity of the PDMS. For the fibrinogen case however, this tendency of losing accumulated molecules is so much reduced so that equilibrium will not be reached over a long time, meaning that it will be possible to accumulate very high concentrations of SLB incorporated molecules. The last statement was not shown in this work but is the theoretically anticipated result which needs to be confirmed by successfully long experiments with fibrinogen barriers.

Theoretically, when the SLB is kept in the center of the channel, the separation profile of accumulated molecules will not be as smeared and as parabolic across the channel as it did for the case without fibrinogen barriers. Also, a more condensed accumulation profile would probably mean no overlap of different accumulated molecules during separation. Although this seems the likely outcome based on previous studies and from the observations made in this work, this result needs to be confirmed experimentally.

Fibrinogen barriers could also be used in another way to separate membrane associated molecules. Figure 5.1.A shows a microfluidic design that could be used to separate two molecules, figure 5.1.B shows the color coding to be used in the description over how separation could be achieved.

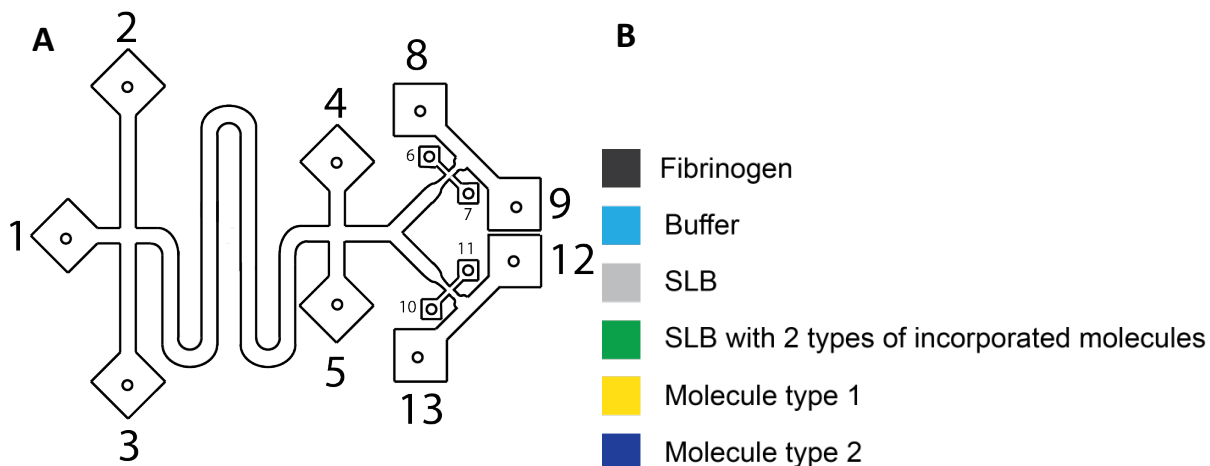


Figure 5.1. (A) Suggested design of microfluidic channel for separating two membrane associated molecules (B) Color coding

Fibrinogen barriers are formed in a number of steps with a result shown in figure 5.2.A. After this has been done an SLB is formed by using for instance 8 as an inlet for the vesicle solution, with buffer simultaneously injected through 1, using 2 and 3 as outlets and keeping all other connections closed, see figure 5.2.B. After appropriate rinsing an SLB plug is formed from vesicles functionalized with two types of incorporated molecules. The vesicle solution could be injected through 4, using 2 and 3 as outlets, injecting buffer through 1. Through adjusting the ratio between vesicle solution and buffer vesicle solution could be flown over an area previously not covered by an SLB, there the vesicles can adsorb to the surface and fuse into an SLB with the two types of incorporated molecules as shown in 5.2.C. A high buffer flow through 1 could then be used to drive the two molecules along the channel using 9 as an outlet. Depending on size the two types will have different velocity, having a long channel then mean that the two types will arrive at the other end at different times. Keeping the buffer flow sufficiently high reduce diffusion during the transport. When the first type of molecule arrive towards connection 8 and 9, it starts to accumulate against the formed fibrinogen barrier. Once accumulation is satisfactory, the bulk flow is stopped and connection 6 is set to suction whilst an air-bubble is switched in through 7 via an electronic switch, all other connections closed. The air-bubble as seen in many experiments completely removes the SLB on its way from 7 to 6, thereby creating a gap in the SLB. This gap ensures that the accumulated molecules have nowhere to diffuse and therefore remain at a high concentration. The driving bulk flow is then started again, but now 12 is used as an outlet and molecule type 2 will start to accumulate against the fibrinogen barrier between 12 and 13. Once accumulated the air-bubble routine can be conducted in a similar fashion, trapping the accumulated molecules in a small area, see figure 5.2.D. The molecules are now separated in two different areas where measurements could be performed, or given the design of the channel. The molecules could also be extracted through flowing some solvent that dissolves SLBs but not fibrinogen, and through some steps vesicles with incorporated molecules could be formed.

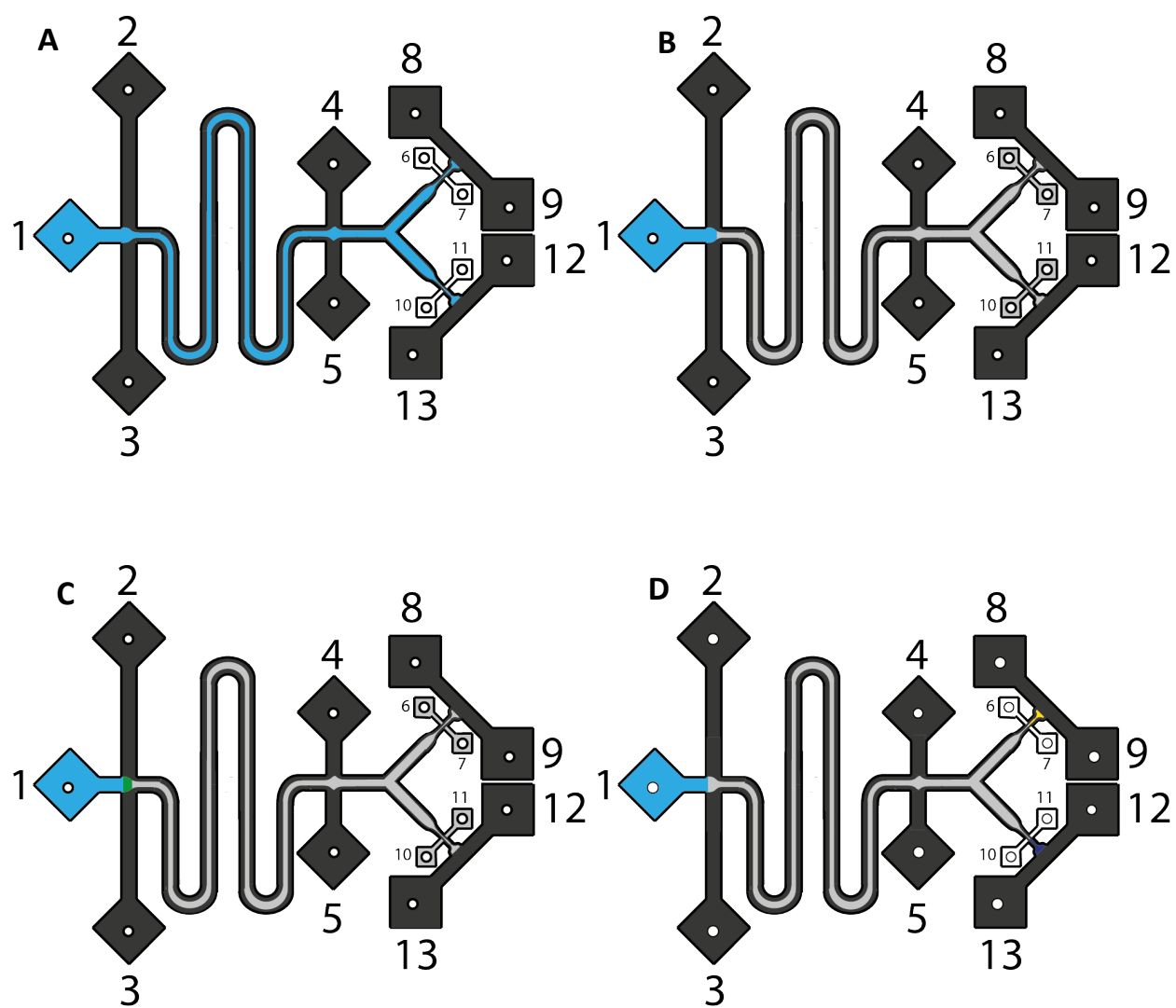


Figure 5.2. (A) Channel with formed fibrinogen barriers (B) SLB formed (C) SLB plug formed (D) Two types of molecules separated in respective arm.

Acknowledgements

I especially want to thank my two supervisors Peter Jönsson and Lisa Simonsson for taking time in the lab, introducing me into the field of microfluidics, epifluorescence microscopy, shear-driven SLBs, answering multitudes of questions, explaining concepts and giving me plenty of support and advice during the whole thesis. A big thank you is due to Fredrik Höök for giving me the opportunity to do this thesis, for good advice during interesting discussions and for solid support. I want to thank Laura de Battice for help performing nanosight measurements and for all other help and valuable advice about lab work that she gave as well as plenty of good discussions. Also I want to thank Björn Johansson, who did his master thesis at the same time as me in the group, for interesting discussions and a lot of terminology.

I'm also grateful to all the coworkers at the Biological Physics department for a willingness to listen, to discuss, to give advice and share good moments.

Last but not least, I want to thank my wife for her untiring love and support and my daughter Mathilda for keeping her spirits high although her father had to leave her on many mornings to conduct this work.

References

1. Phillips, R., J. Kondev, and J. Theriot, *Physical Biology of the Cell* 2009, Abingdon: Garland Science.
2. Alberts, B., et al., *Essential Cell Biology*. 3rd Edition ed 2010, London: Garland Science.
3. Overington, J.P., B. Al-Lazikani, and A.L. Hopkins, *How many drug targets are there?* Nat Rev Drug Discov, 2006. **5**(12): p. 993-996.
4. Hopkins, A.L., J.S. Mason, and J.P. Overington, *Can we rationally design promiscuous drugs?* Current Opinion in Structural Biology, 2006. **16**(1): p. 127-136.
5. Jönsson, P., et al., *Shear-Driven Motion of Supported Lipid Bilayers in Microfluidic Channels*. Journal of the American Chemical Society, 2009. **131**(14): p. 5294-5297.
6. Jönsson, P., A. Gunnarsson, and F. Höök, *Accumulation and Separation of Membrane-Bound Proteins Using Hydrodynamic Forces*. Analytical Chemistry, 2010. **83**(2): p. 604-611.
7. Jönsson, P., et al., *Mechanical Behavior of a Supported Lipid Bilayer under External Shear Forces*. Langmuir, 2009. **25**(11): p. 6279-6286.
8. Jönsson, P. and F. Höök, *Effects of Surface Pressure and Internal Friction on the Dynamics of Shear-Driven Supported Lipid Bilayers†*. Langmuir, 2010. **27**(4): p. 1430-1439.
9. Simonsson, L., et al., *Continuous lipid bilayers derived from cell membranes for spatial molecular manipulation* 2011, Applied Physics: Gothenburg.
10. *Lissamine™ rhodamine B 1,2-dihexadecanoyl-sn-glycero-3-phosphoethanolamine, triethylammonium salt (rhodamine DHPE)*. [cited 2011 05-29]; Available from: <http://products.invitrogen.com/ivgn/product/L1392>.
11. Jönsson, P., *Using Photobleaching to Characterize the Mobility of Membrane-Associated Molecules*, in *Solid State Physics* 2008, Lund University: Lund.
12. Groves, J.T. and S.G. Boxer, *Micropattern Formation in Supported Lipid Membranes*. Accounts of Chemical Research, 2002. **35**(3): p. 149-157.
13. Richter, R.P., J.L.K. Him, and A. Brisson, *Supported lipid membranes*. Materials Today, 2003. **6**(11): p. 32-37.
14. Koenig, B.W., et al., *Neutron Reflectivity and Atomic Force Microscopy Studies of a Lipid Bilayer in Water Adsorbed to the Surface of a Silicon Single Crystal*. Langmuir, 1996. **12**(5): p. 1343-1350.
15. Johnson, S.J., et al., *Structure of an adsorbed dimyristoylphosphatidylcholine bilayer measured with specular reflection of neutrons*. Biophysical journal, 1991. **59**(2): p. 289-294.
16. Bayerl, T.M. and M. Bloom, *Physical properties of single phospholipid bilayers adsorbed to micro glass beads. A new vesicular model system studied by 2H-nuclear magnetic resonance*. Biophysical journal, 1990. **58**(2): p. 357-362.
17. Jönsson, P., *Properties and Applications of Shear-Driven Lipid Bilayers*, in *Applied Physics* 2010, Chalmers University of Technology: Gothenburg.
18. Jönsson, P., M.P. Jonsson, and F. Höök, *Sealing of Submicrometer Wells by a Shear-Driven Lipid Bilayer*. Nano Letters, 2010. **10**(5): p. 1900-1906.
19. Groves, J.T. and S.G. Boxer, *Electric field-induced concentration gradients in planar supported bilayers*. Biophysical journal, 1995. **69**(5): p. 1972-1975.
20. Hovis, J.S. and S.G. Boxer, *Patterning Barriers to Lateral Diffusion in Supported Lipid Bilayer Membranes by Blotting and Stamping*. Langmuir, 2000. **16**(3): p. 894-897.
21. Groves, J.T., N. Ulman, and S.G. Boxer, *Micropatterning Fluid Lipid Bilayers on Solid Supports*. Science, 1997. **275**(5300): p. 651-653.

22. Simonsson, L., et al., *Site-Specific DNA-Controlled Fusion of Single Lipid Vesicles to Supported Lipid Bilayers*. ChemPhysChem, 2010. **11**(5): p. 1011-1017.
23. Mester, A.J., *Blood Plasma Fibrinogen in Rheumatic and Non-Rheumatic conditions*. Ann Rheum Dis. , 1945. **4**(3): p. 57–59.
24. Slayter, C.E.H.a.H.S., *The Fibrinogen Molecule: Its Size, Shape, and Mode of Polymerization*. J Biophys Biochem Cytol. , 1959. **5**(1): p. 11–27.
25. Toscano, A. and M.M. Santore, *Fibrinogen Adsorption on Three Silica-Based Surfaces: Conformation and Kinetics*. Langmuir, 2006. **22**(6): p. 2588-2597.
26. Beijbom, L., et al., *Structure analysis of fibrinogen by electron microscopy and image processing*. Journal of Ultrastructure and Molecular Structure Research, 1988. **98**(3): p. 312-319.
27. Sigma-Aldrich. *F3879 Fibrinogen from human plasma*. 2011 [cited 2011 2011-05-13]; Available from:
http://www.sigmaaldrich.com/catalog/ProductDetail.do?N4=F3879|SIGMA&N5=SEARCH_CONCAT_PNO|BRAND_KEY&F=SPEC.
28. Salim, M., et al., *Characterization of fibrinogen adsorption onto glass microcapillary surfaces by ELISA*. Lab on a Chip, 2007. **7**(1): p. 64-70.
29. Whitesides, G.M., *The origins and the future of microfluidics*. Nature, 2006. **442**(7101): p. 368-373.
30. Alonso Marcelo , F.E.J., *Physics*. 1 ed1992, Harlow: Addison-Wesley Publishing Company.
31. Jönsson, P., et al., *A Method Improving the Accuracy of Fluorescence Recovery after Photobleaching Analysis*. Biophysical journal, 2008. **95**(11): p. 5334-5348.

Appendix A - Manufacturing microfluidic channels

1. Weigh 4g PDMS (Sylgard 184) and 0.4g of curing agent in a plastic container, stir for a couple of minutes with the tip of a pipette in order to mix thoroughly.
2. Put the container in a vacuum chamber in order to subtract all gas from the PDMS mould for about 15 minutes.
3. Clean the master gently with some N₂ gas; place the master on the lid of a flask. Pour the PDMS over the master, start outside of the channels and pour it in an overlapping manner in order to reduce the risk of encapsulating air bubbles in the PDMS.
4. Bake in an oven at approximately 95°C for about one hour.
5. Clean two glass substrates (nr.1 ~0.16mm thick) in TL1 solution (5 parts MilliQ water, 1 part 25% NH₃, 1 part 30% H₂O₂). Place two small beakers in a fume hood on a heating plate, 10ml MilliQ water was added to each together with 2ml NH₃ and 2ml H₂O₂. One glass substrate was put into each beaker and the temperature was set to ~140°C and left for 15 minutes. Pick up the substrates with tweezers and remember which side was facing upwards in the beaker, rinse thoroughly with MilliQ water, leave in a clean beaker filled with MilliQ for about 15 minutes, dry with N₂, switch grip and dry again with N₂.
6. Put in an oven at 150°C for about thirty minutes.
7. Put the glass substrates in a shallow beaker and put it into the plasma oven. Close front valve and start vacuum pump, wait until silence, set for high, turn on oxygen and use front valve 2 to regulate the amount of oxygen in the oven. When regulating the light in the oven passes a pink spectrum and turns into a bluish-/whitish tint. Let the substrates remain in the oven for about fifteen minutes (bring the glass substrates to the PDMS lab in a disposal plastic container in order not to bring back any PDMS back into the biochemical lab).
8. Take out the master with the PDMS-cast; gently peel along the edge of the master with tweezers in order to loosen the PDMS from it, when starting to detach lift carefully until separated. Put the PDMS cast on a bigger glass substrate, use a sharpened cylinder (~1.2mm diameter) to perforate holes into each reservoir. Cut away any excessive PDMS material, turn up-side-down and put in a plasma oven, almost 2/3rds towards the rear end of the oven. Press the oven lid and start the vacuum pump, put the oven on high and open O₂ valve. Regulate the O₂ as before by turning the valve between oven and vacuum pump past pink tint until dark purple/blue. Leave for about 30s, too long will make PDMS brittle and to short time results in poor bonding.
9. Put the cleaned glass substrates on a paper with the clean side up, mount the cleaned PDMS with a set of tweezers and press gently.
10. Put in an oven and let it bond ~95°C for 5 minutes. Check that the PDMS has bonded to the substrate by trying to separate them with tweezers.
11. Fill the microfluidic channels by putting a drop of water at one of the reservoirs (keeps them hydrophilic for a longer time).

12. Take another substrate and put some glue on it inside the fume hood. Cut silicone tubing into ~1cm long parts. Rinse each tube with a drop of water and blow-dry them (use a self-closing tweezers).
13. Use a pipette tip to put glue along the edge of a silicone tube before mounting it over the opening of a reservoir and press gently. Hold up, without tilting, against the light and check that the tube is centered over the opening, otherwise adjust it.
14. Leave in the fume hood with a small container with water close to it and put a bigger container up-side-down over it and let it rest for 45-60 minutes.
15. Check that solution could pass through each inlet with a pipette and open any reservoirs that have been clogged by glue with a syringe needle and recheck.
16. Keep refrigerated in a tube with MilliQ water.

Appendix B - Preparation of lipid vesicles

A round-bottom flask was first rinsed with some methanol. In order to produce vesicles with 0.1 wt% R-DHPE 0.5ml methanol was first added together with 99 μ l POPC (25 mg/ml) and 10 μ l R-DHPE (2.5 mg/ml). The solution was thoroughly mixed by vibration for about two minutes. The flask was sealed with a rubber strut and two syringe needles were inserted through it. The methanol was then evaporated in a fume hood with nitrogen (N₂) while rotating the flask. After this the flask was dressed in aluminum foil, to prevent bleaching of the rhodamine. It was then left in the fume hood and flowed with N₂ as before for about one hour, this in order to ensure complete evaporation of the methanol as it if left would act to dissolve formed vesicles. The flask was then filled with 1ml buffer (100mM NaCl, 10mM and mixed through vibration for about two minutes. Two glass syringes with a 30 nm filter membrane were coupled in a extruder setup. The solution was put into one of the syringes after which the solution was extruded 13 times back and forth through the membrane. The vesicle solution was then put in a 2ml vial, briefly flooded with N₂ before sealing, labeled and dressed in aluminum foil before it was put for storage in a fridge.

Appendix C - Switching used in the experiments

